Cite this article
Ong YH, Toh CT, Chee SK and Mohamad H
Bored piles in tropical soils and rocks: shaft and base resistances, *t–z* and *q–w* models.
Proceedings of the Institution of Civil Engineers – Geotechnical Engineering,
https://doi.org/10.1680/jgeen.19.00106

Research Article
Paper 1900106
Received 03/05/2019;
Accepted 23/03/2020

Keywords: field testing & monitoring/ piles & piling/rocks/rock mechanics

Geotechnical Engineering

ice Publishing

Bored piles in tropical soils and rocks: shaft and base resistances, *t–z* and *q–w* models

1 Yin Hoe Ong BEng, MEng
Director, Dr Toh Associates Sdn Bhd, Geotechnical Consultant, Kuala Lumpur, Malaysia; PhD candidate, Department of Civil & Environmental Engineering, Universiti Teknologi Petronas, Bandar Seri Iskandar, Perak, Malaysia (corresponding author: drtohassociates@gmail.com)

2 Cheng Teik Toh BEng, PhD, CEng, MICE
Director, Dr Toh Associates Sdn Bhd, Geotechnical Consultant, Kuala Lumpur, Malaysia

3 Sai Kim Chee BSc
Director, Dr Toh Associates Sdn Bhd, Geotechnical Consultant, Kuala Lumpur, Malaysia

4 Hisham Mohamad BEng, MSc, DIC, PhD
Associate Professor, Department of Civil & Environmental Engineering, Universiti Teknologi Petronas, Bandar Seri Iskandar, Perak, Malaysia



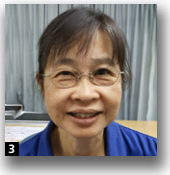


Analyses of load tests on 100 instrumented bored piles in different weathering grades of different tropical geological formations of peninsular Malaysia enabled correlations of ultimate shaft and base resistance with standard penetration test (SPT) results and unconfined compression strengths. The data also enabled development of shaft resistance (*t–z*) and base resistance (*q–w*) models that are related to SPT, unconfined compressive strength and rock types. The *t–z* models can be used for strain softening and strain hardening while the *q–w* models are for strain hardening and stiffening behaviour. The models thus developed were applied for analysis of 35 piles in the database that were loaded until the load–settlement curves were significantly non-linear. Most of the analyses resulted in a reasonable match with the measured load–settlement and load-transfer curves up to 1.5 times the pile working load, regardless of whether the *q–w* function was strain hardening or stiffening. Accurate matching with measured load–settlement and load-transfer curves for 1.5–3 times working load was conditional on the correct choice of the *q–w* function. The models were further tested against 27 published load test results from across the world.

Notation

A	coefficient relating f_{bu} to q_u, G to N and q_{max} to q_u
B	coefficient relating G to N
C_u	undrained shear strength
f_b	base resistance (kPa)
f_{ba}	allowable base resistance
f_{bu} or q_{max}	ultimate base resistance
f_s	pile shaft friction
f_{sa}	allowable shaft resistance
f_{su}	ultimate shaft resistance
G	shear modulus
IGM	Intermediate Geomaterials – appears in Figs 2–5
K_b	coefficient relating ultimate base resistance to standard penetration test (SPT) N
k_{ib}	initial stiffness of strain hardening q–w curve (kPa/mm)
k_{ib2}	stiffness at higher toe settlement of stiffening q–w curve (kPa/mm)
k_{is}	initial stiffness of t–z curve (kPa/mm)
K_s	coefficient relating ultimate shaft resistance to SPT N
l	pile length
n	number of samples and a variables in Tsai model
p_a	atmospheric pressure, 100 kPa
q	base resistance
q_u	unconfined compressive strength
R	constant in Ramberg and Osgood model that controls the curvature of the ascending curve. Higher R increases the curvature; see Figure 13
r	constant in Tsai model that controls the curvature. Higher r values result in higher degrees of strain softening; see Figure 13
r_m	distance where shear stress becomes negligible, $r_m = 2.5\ l\ (1 - v)$ where l pile length
r_0	radius of pile
r^2	coefficient of determination
N	blow count in SPT
T	constant that influences the curvature of the curve. Higher T increases the curvature. $T > 1$ for strain hardening q–w curve and $0 < T < 0$ for stiffening q–w curve; see Figure 14
t	shaft resistance
$\sigma_{\bar{X}}$	standard error
α	constant in Ramberg and Osgood model that controls the displacement at f_{su}. Higher α increases the displacement at f_{su}; see Figure 13

α, α_q	coefficients relating f_{su} to q_u (Seidel and Collingwood, 2001)
α_c	coefficient relating f_{su} to C_u (Kulhawy and Phoon, 1993)
β	constant that influences the pile toe settlement at f_{bu}. Higher β increases the pile toe settlement at f_{bu}; see Figure 14.
δ_s or z	shaft displacement
δ_{su}	shaft displacement at f_{su}
δ_b or w	pile toe settlement / pile diameter (%)
ν	Poisson's ratio
ψ, β	coefficient relating α_c to q_u / $2P_a$ (Kulhawy and Phoon, 1993)

1. Introduction

One hundred instrumented test piles were analysed to obtain correlations of ultimate shaft and base resistance with strength. These piles were instrumented and either loaded at the top in the conventional manner of maintained load tests or by use of bi-directional load cells. The piles were constructed through different weathering grades of clastic and non-clastic sedimentary, meta-sedimentary, metamorphic and granite rocks of peninsular Malaysia. The list and salient features of the test piles are summarised in Appendix 1.

Correlations of ultimate shaft resistance with strength for the entire weathering profile from grade VI to grade I of the different geological formations were obtained from the results. There is a broad trend in the correlations, similar to those published by others, but as would be expected there is also appreciable scatter. Only five piles were loaded until ultimate pile capacity, which is defined as when the ultimate shaft and ultimate base resistances have been fully mobilised and at which load the pile settlement will continue unabated.

Strain-softening shaft behaviour was found to be prevalent for standard penetration test (SPT) N values of up to 30, whereas strain-hardening behaviour was more common for higher strengths. For shaft resistance, the Tsai (1988) function originally developed for concrete and the Ramberg and Osgood (1943) function for alloys were adapted for use as shaft resistance–vertical displacement (t–z) curves for strain-softening and strain-hardening behaviour, respectively. For base resistance, the measured base resistance–base displacement (q–w) curves are either linear elastic with strain hardening or that which stiffens with increasing pile toe pressure. The Ramberg and Osgood model was used to model both types of q–w curves. Characteristic t–z and q–w models were developed for different SPT N and q_u values representative of the entire spectrum of weathering, with strengths from stiff to very hard and from very weak to moderately strong, as well as different rock types.

These models were then tested to compare the full axial compression load–settlement curve and load-transfer curves for 35 instrumented test piles from the database and subsequently tested against 27 published test results from across the world. The results are encouraging, with most analyses resulting in a reasonable match with the measured load–settlement and load-transfer curves up to 1.5 times the pile working load, regardless of whether the q–w function was strain hardening or stiffening. Accurate matching with measured load–settlement and load-transfer curves beyond 1.5 times working load and until 3 times working load was conditional on the correct choice of the q–w function.

In this paper the term soil is applied to unconsolidated sediments, for example, tin tailings and alluvial deposits and completely weathered rock (grade VI of the weathering profile). Other materials of the weathering profile will be described as rock of the appropriate weathering grade (grade I to grade V).

2 Geological formations

All the piles were in the three main rock formations, as follows

(*a*) clastic sedimentary and meta-sedimentary rocks that occur over about 40% of the land area of peninsular Malaysia and include shales, siltstones, sandstones, mudstones, gneiss, schists and phyllites; these rocks are often highly folded and fractured
(*b*) igneous intrusions, mainly granite and some intermediate to basic rocks, that occur over about 40% of the land mass of peninsular Malaysia
(*c*) limestone in the capital city Kuala Lumpur, Ipoh and Kuching cities.

The weathering classification scheme adopted in this paper follows that by the Geological Society Engineering Group Working Party (EGGS, 1990). Depth of weathering can extend to more than 40 m. Weathering profiles in sedimentary formations are more complex than granite formations due to inhomogeneity (layering) and textural variations of the rock. Table 1 gives typical depths and thicknesses of the different weathering horizons in igneous and sedimentary formations.

Limestone, a non-clastic sedimentary rock, has particular characteristics that differentiate it from clastic sedimentary rocks. Despite the fact that its spatial occurrence is far less widespread than granites and sedimentary rocks, limestone is of significance in that it occurs over commercially important parts of the capital city. The nature of the limestone is described by Yeap (1985). A range of soil types are found above limestone and include alluvium, tin tailings, weathered clastic sedimentary and metamorphic rocks. Granite intrusions can occur next to limestone. The properties of the weathered granite and sedimentary formations can be severely affected by proximity to limestone. In contact zones between limestone and granite, the depth to limestone rock can exceed 100 m (Yeap, 1985).

3. Bored piles in different geological formations

Bored piles in sedimentary clastic and metamorphic formations are very commonly constructed through the weathering

Table 1. Typical weathering profiles

Igneous	Clastic sedimentary
Thickness of grade VI and V vary up to 20 m	Grade VI is generally thin and of the order of 5 m Thickness of grade V is of the order of 5 to 10 m
Thickness of grade IV can be about 10 m Depth to grade III can be about 30 m to 40 m Thickness of grade III is about 10 m	Grade IV and III are relatively thick and often greater than 20 to 30 m
Depth to grade II often between 40 m to 50 m	Grade II is often more than 40 m deep

profile from grade VI to grade III, deriving most of the shaft resistance from the weathered rocks that transcend from very stiff ($15 < \text{SPT } N < 30$), to hard ($30 < \text{SPT } N < 50$) to very hard soils (SPT $N > 50$) or extremely weak ($q_u < 0.6$ MPa), very weak ($0.6 < q_u < 1.25$ MPa), weak ($1.25 < q_u < 5.0$ MPa) and moderately weak ($5.0 < q_u < 12.5$ MPa) rocks. The very weak to moderately weak rocks are commonly highly fractured.

Bored piles in granites commonly extend through the weathering profile (grade VI to grade III) and socketed into grade I and II rocks. Bored piles in limestone, with alluvium, tin tailings, clastic sedimentary and metamorphic rocks above the limestone are often socketed into moderately weathered (grade III) to fresh (grade I) limestone rock.

4. Standard penetration test for weathering grades III to VI

The friable nature of the soils and extremely weak to moderately weak rocks prevents recovery of a suitable size undisturbed samples for laboratory strength tests. Attempts at recovering samples using retractable type triple tube core barrels very often result in poor recovery and highly fractured samples that cannot be used for unconfined compression tests. Hence, and in view of heterogeneity that can be severe, design procedures are based on the standard penetration test (SPT); larger numbers of boreholes with SPTs are preferred to fewer boreholes with pressuremeter tests and recovery of intact samples for laboratory strength tests. The cost of a pressuremeter test is about ten times the cost of a SPT.

The strengths of the very hard soils and extremely weak to moderately weak rocks are higher than that corresponding to SPT N of 50/300 mm penetration. The practice of determining the N value is not by dropping the hammer repeatedly until 300 mm penetration, but rather by measuring the penetration of the hammer up to 50 blows and linearly extrapolating the SPT N in the manner described by Thompson and Leach (1988). Attempts at repeated blows to achieve a 300 mm penetration are not carried out as it almost invariably leads to damage to the SPT sampler as well as to the rods.

Stroud (1974) showed that the ratio of C_u to SPT N is between 4 and 6, with the higher coefficient for lower plasticity index of less than 20%. Wong and Singh (1996) reported an average ratio of 4 for sedimentary formations around Kuala Lumpur with plasticity index of between 20 and 30%. The plasticity index values for grades III to VI granites and siltstones and sandstones are typically between 10 and 20%. Following Stroud (1974), the ratio would be close to 5. The use of the ratio in this paper is only to enable comparison of shaft and base resistance factors and shear modulus that are related to SPT N with the data from Kulhawy and Phoon (1993), Zhang and Einstein (1998) and others that are related to C_u or q_u.

5. Local methods of pile construction and shaft roughness

Soil auger and soil boring buckets are commonly used to bore through hard and very hard soils and extremely weak and very weak rocks; the former for dry and the latter for wet conditions. Tapered soil augers equipped with round shank chisels are commonly used to bore through very weak and weak rock. Core barrels with round shank chisels are used for weak rock, moderately weak rocks and moderately strong rocks. Often for moderately strong and strong rock the entire rock core is retrieved by the core barrel; rougher surfaces result when roller bits are used. If the core cannot be retrieved using a core barrel, a cross-cutter is used to break the rock after a ring has been cut by the core barrel. Core barrels with roller bits followed by cross-cutters are used for strong and very strong rocks.

Stabilisation of pile borings is often by use of a relatively short casing, commonly between 6 and 12 m, with drilling fluid often being water, bentonite or polymer. Base cleaning is most often by repeated use of a cleaning bucket. Other methods in use include air lifting or a submersible sand pump, which also serves the purpose for de-sanding and re-circulating bentonite. When polymers are used in silty soils, a coagulant is sometimes added to accelerate sedimentation, followed an hour later by repeated use of a cleaning bucket to remove the coagulated sediments. Concreting is by the tremie method, even if the pile boring is dry. Direct discharge of concrete into a dry hole is not encouraged as experience has it that lower shaft resistances result.

An assessment of pile shaft roughness for piles installed in the manner described above was carried out by measuring the surfaces of contiguous bored piles exposed during basement excavation. The measured roughness falls within the bounds by

Seidel and Collingwood (2001) and is in the range of mostly 3–17 mm, corresponding to a roughness class that is mostly R3 but also R4, following the classification by Pells (1999).

6. Design equations and parameters

6.1 Shaft resistance

The two common shaft resistance equations are:

$$f_{su}(\text{kPa}) = K_s N$$

and

$$f_{su} = \alpha q_u^{\beta} = \alpha_q q_u$$

Seidel and Collingwood, 2001) with $\alpha_q = \alpha q_u^{\beta-1}$

Relating α_q to K_s requires assuming a correlation between C_u and N. Assuming C_u (kPa) = $5N$ or q_u (kPa) = $10N$ leads to the following convenient equation.

$$\alpha_q = K_s/10$$

The K_s values that are commonly adopted for design in Malaysia are given in Table 2. For weak rocks of weathering grades III and IV, the highest SPT N value is limited to 150 or 200. Malaysia does not have a foundation code that stipulates the K_s values for design. However, the Singapore foundation code CP4 (SSC, 2003) recommends K_s of between 1.5 and 3.0 and limiting the ultimate shaft resistance to 150 kPa for clays and 300 kPa for sands and cemented soils. The use of K_s of 2.5 is the same as adopting a pile adhesion factor of 0.5 for bored piles in clay (Fleming *et al.*, 2008) and assuming $C_u = 5N$.

6.2 Base resistance

The ultimate base resistance is given by

$$f_{bu}(\text{kPa}) = K_b N$$

K_b of 30 is commonly adopted in design.

Assuming a factor of safety of 3 for base resistance.

$$f_{ba} = 30N/3 = 10N$$

Table 2. Commonly adopted design parameters

SPT N along the pile shaft	Maximum permissible K_s
<10	3.5
11 < N < 50	3.0
51 < N < 100	2.5
101 < N < 150	2.0

Assuming $C_u = 4N$, $5N$ and $6N$ leads to f_{ba} of $1.25q_u$, $1.0q_u$ and $0.83q_u$, respectively. This is in line with the proposals by Rowe and Armitage (1987) and Fleming *et al.* (2008) to adopt the expression:

$$f_{ba} = q_u$$

7. Instrumented test piles

All the bored piles were instrumented using vibrating wire strain gauges or the Glostrext displacement gauges (Hanifah and Lee, 2006), which measure pile shortening rather than strains. Telltales are often included to check the settlements computed from integration of strains. These piles were tested in the different geological formations throughout peninsular Malaysia between the years 1990 and 2018. Resistant wire strain gauges were used for pile instrumentation until about 1998. Vibrating wire gauges and the Glostrext system have been in use since 1998 and 2004, respectively.

In all cases a borehole with SPT is located close to the pile, thereby enabling correlations of the shaft and base parameters with SPT N values. However, in the case of piles in grade I, II and III rock, although the rock quality designations (RQDs) were recorded in the borehole next to the test pile, unconfined compression tests were not always carried out. In this paper, correlations with unconfined compression strength were made only if the test was carried out next to the pile.

8. Shaft resistance from test piles

8.1 K_s plotted against SPT N

Figure 1 is the plot of all the shaft resistance parameters K_s (f_{su}/N) from the strain and displacement gauges. The data

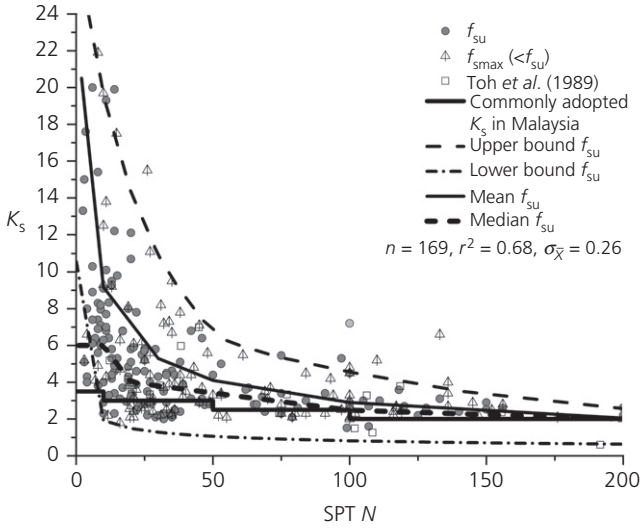

Figure 1. Measured K_s plotted against SPT N

plotted include the ultimate shaft resistance, as well as the maximum mobilised values where the ultimate shaft resistance had not been reached ($K_s = f_{smax}/N$). However, only the shaft friction coefficients calculated from f_{su}, totalling 169 data points, are included in the derivation of the empirical equations and the mean, median, lower bound and upper bound lines. The limited data by Toh *et al.* (1989) are included and found to be in good agreement. The trend is one of reducing K_s values with increasing SPT N with K_s ranging from 5 to 20 at low SPT N of less than 10 to about 2 for SPT N of 100 to 200. The parameters commonly adopted in Malaysia are included therein and are shown to be conservative.

Mean and median are included in Figure 1. The mean is from linear regression analysis, whereas the median is estimated separately for small intervals of SPT N values. The difference between mean and median values for SPT N greater than 50 is small. For SPT N less than 50, the median line is below the mean.

Figure 2 is the plot of K_s against N on log scales. The lower bound (visually determined), mean (linear regression) and upper bound (visually determined) lines of the yielded points can be approximated by:

$$\text{Lower bound}: K_s = 8\ \text{SPT}\ N^{-0.5}$$

$$\text{Mean}: K_s = 29\ \text{SPT}\ N^{-0.5}$$

$$\text{Upper bound}: K_s = 88\ \text{SPT}\ N^{-0.5}$$

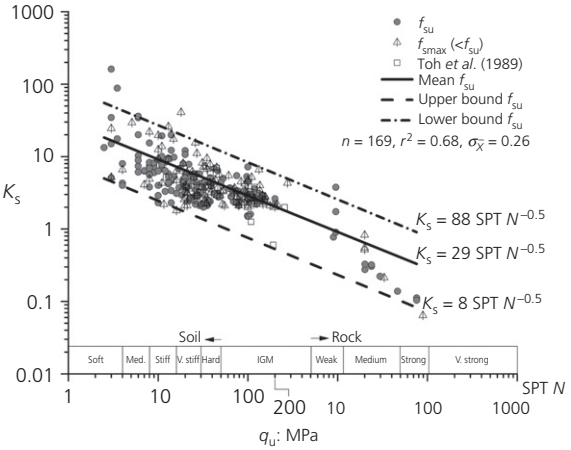

Figure 2. Measured K_s plotted against SPT N log-log scale

8.2 α_c and α_q against q_u

Figure 3 shows the authors' data (assuming $C_u = 5N$) plotted as α_c against $q_u/2P_a$ compared with the data by Kulhawy and Phoon (1993). The data of Kulhawy and Phoon (1993) showed two distinct trend lines: an upper band for rocks extending from q_u of about 0.4 to about 80 MPa and a lower band for clays with q_u from about 0.04 to 0.6 MPa. Kulhawy and Phoon (1993) proposed a general equation for piles:

$$\alpha_c = \psi(q_u/2P_a)^{-\beta}$$

with $\beta = 0.5$ and ψ of 0.5 for clay and between 1.0 and 3.0 for rocks.

The authors' data fall above Kulhawy and Phoon's data for clay, but follow their general trend line for rock. The authors' data are also plotted as α_q against q_u and compared with those by Kulhawy and Phoon (1993) in the manner presented by Seidel and Collingwood (2001) in Figure 4, assuming $C_u = 5N$. The data presented in Figures 3 and 4 show that the trend line for rock established by Kulhawy and Phoon (1993) from weak to strong rock is similar to that from the authors' data for firm to hard soils (grade VI) and weathered rock of grades I to V. Broadly the same correlation of ultimate shaft resistance with strength holds for the full strength range from 0.02 to 80 MPa, albeit with scatter, and can be represented by the following equations:

$$\text{Lower bound } \alpha_q = 0.08q_u^{-0.5} \text{ corresponding to } \psi = 0.36 \text{ and } \beta = 0.5$$

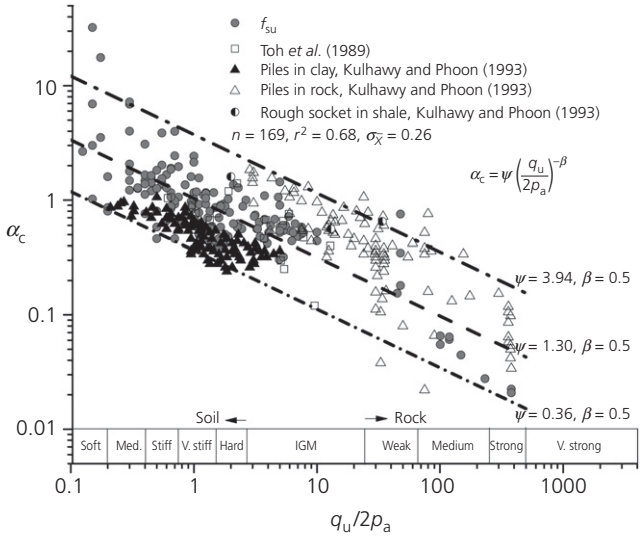

Figure 3. Measured and Kulhawy and Phoon's α_c plotted against normalised q_u

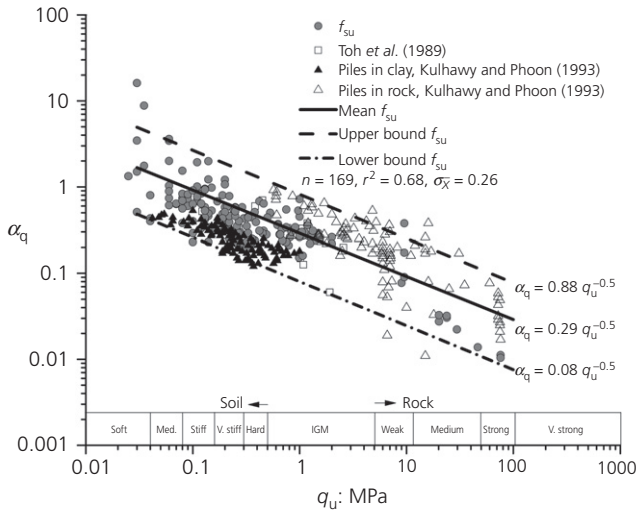

Figure 4. Measured and Kulhawy and Phoon's α_q plotted against q_u

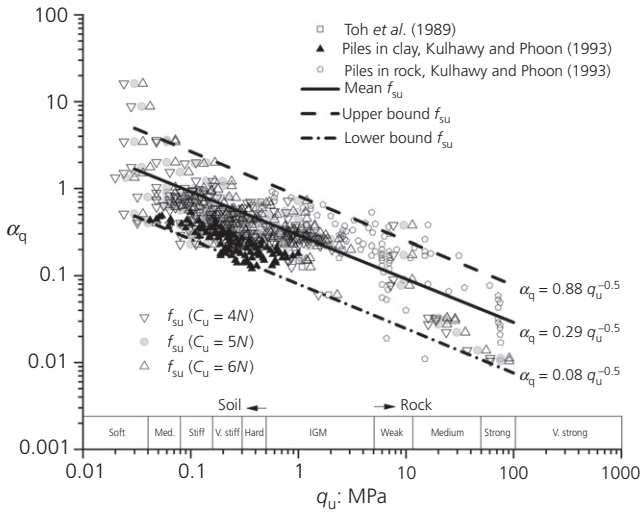

Figure 5. Measured and Kulhawy and Phoon's α_q against q_u plotted for $C_u = 4N$, $5N$ and $6N$

$$\text{Mean } \alpha_q = 0.29 q_u^{-0.5} \text{ corresponding to } \psi = 1.30 \text{ and } \beta = 0.5$$

$$\text{Upper bound } \alpha_q = 0.88 q_u^{-0.5} \text{ corresponding to } \psi = 3.94 \text{ and } \beta = 0.5$$

where the upper and lower bound lines were visually determined and the mean from linear regression.

The coefficient of determination and standard error of the mean line in Figures 2–4 are 0.68 and 0.26, respectively, compared to Kulhawy and Phoon's coefficient of determination of between 0.461 to 0.768 and standard error of 0.089 to 0.252.

Figure 5 is the same plot as Figure 4 except that different correlations $C_u = 4N$, $5N$ and $6N$ are all used. The purpose is to demonstrate that the different correlations do not have a significant effect on the lower bound, mean and upper bound relationship between α_q and q_u.

The α and β values are compared to those by others as summarised by Seidel and Collingwood (2001) in Table 3.

Table 3. Comparison of parameters α and β

Design method	α	β
Horvath and Kenny (1979)	0.31	0.50
Carter and Kulhawy (1988)	0.20	0.50
Williams *et al.* (1980)	0.44	0.36
Rowe and Armitage (1984)	0.40	0.57
Rosenberg and Journeaux (1976)	0.34	0.51
Reynolds and Kaderbeck (1980)	0.30	1.00
Gupton and Logan (1984)	0.20	1.00
Reese and O'Neill (1988)	0.15	1.00
Toh *et al.* (1989)	0.25	1.00
This paper lower bound	0.08	0.50
This paper mean	0.29	0.50
This paper upper bound	0.88	0.50

9. Base resistance from test piles

Of the 100 piles only 12 piles were loaded until the base pressure reached the ultimate base capacity or a pile toe displacement of 4.5% pile diameter (following the criteria by Ng *et al.* (2001) for piles in saprolites and other weathered rock in Hong Kong). Pells (1999) reported that ultimate base capacities are attained at displacements exceeding 5% of the pile diameter. Williams and Pells (1981) showed that the ultimate base resistance can exceed $10q_u$ for pile embedment exceeding five pile diameters.

K_b from defining ultimate base resistance as either ultimate pile capacity or the pressure corresponding to pile toe displacement of 4.5% are plotted against SPT N in Figure 6; the K_b values range from 20 to 90. Zhang and Einstein (1998) showed that the ultimate base resistance can be represented by:

$$f_{bu} = A(q_u)^{0.5}$$

with $A = 6.6$, 4.8 and 3.0 for the upper bound, mean and lower bound, respectively.

The authors' data are plotted against the bounds by Zhang and Einstein (1998) in Figure 7 assuming $C_u = 4N$, $5N$ and $6N$. The upper bound is similar to that by Zhang and Einstein but

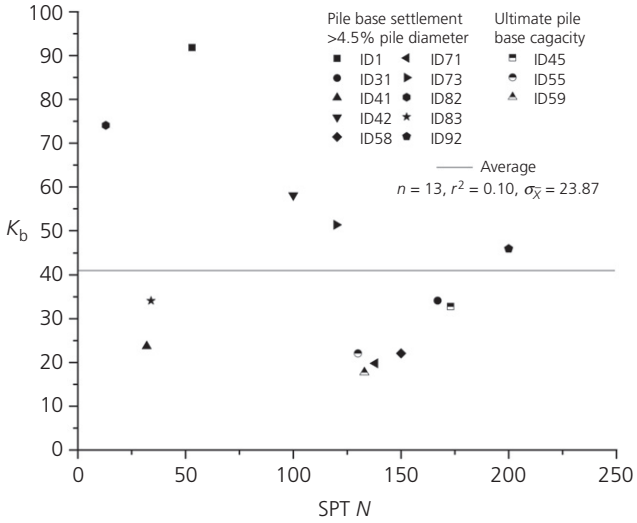

Figure 6. Measured K_b plotted against SPT N

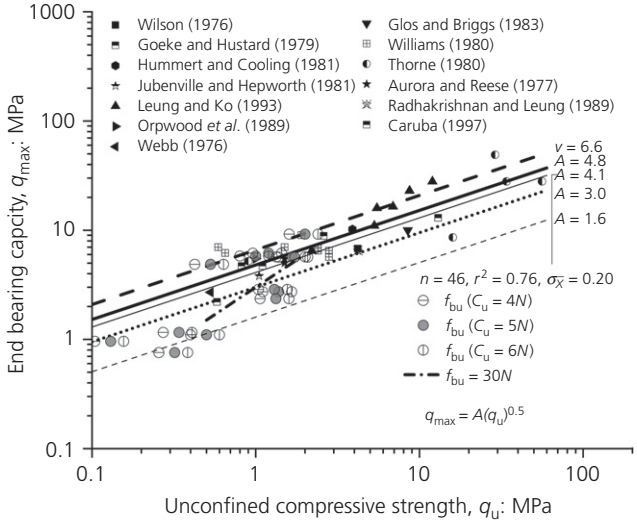

Figure 7. Measured pile base resistance plotted against q_u

the lower bound line is appreciably lower, corresponding to A of 1.6 and a mean line corresponding to A of 4.1. The coefficient of determination and standard error of the mean line are 0.76 and 0.20. The different assumptions of C_u/N have little effect on the relationships between f_{bu} and q_u.

The K_b value of 30 that is referred to in Section 6.2 is plotted onto Figure 7. The $K_b = 30$ line spans across the lines corresponding to $A = 1.6$ for q_u of 0.5 MPa to $A = 4.1$ for q_u of 2.0 MPa.

10. *t–z* and *q–w* curves from test piles

Figures 8(a)–8(e) and 9(a)–9(e) are the shaft resistance–shaft displacement curves for different SPT N categories and rock types, respectively, directly from the strain gauges or displacement gauges in the test piles. The shaft settlement $\delta_s(z)$ is the total settlement at the same level as the shaft friction $f_s(t)$ and is obtained by integration of the measured strains with measured top displacement as an end condition. Shaft friction is obtained from equilibrating the side shear force with the difference in the axial loads from the strain gauges between two gauge levels. The pile modulus is the applied normal stress divided by the vertical strain measured close to the point of load application. The results are presented directly as calculated from the strain gauges without curve smoothening and curve fitting the data points. It is not possible to normalise the vertical axis by plotting f_s/f_{su}, because this would require that all the $t–z$ curves had reached f_{su},- which is not the case for a significant number of the measured curves. Normalising the horizontal axis against the pile diameter was attempted, but this did not help to reduce the scatter.

Different shades are used for work softening curves to distinguish from perfect plasticity and strain hardening behaviour. As summarised in Table 4, strain softening behaviour was observed for a majority of the cases where SPT N was less than 30. The proportion exhibiting strain softening decreases with increasing strength except when the strength exceeds 6 MPa. For almost all strain hardening $t–z$ curves, there is no distinct yield stress. The degree of strain softening (the percentage reduction in strength after yield) is of the order of 40% for materials with SPT N of less than 10 and about 30% for materials with SPT N of 10 to 30.

The loads reaching the pile toe for many of the tested piles are relatively low and therefore many of the measured $q–w$ curves are within the elastic range. However, there is sufficient information to show two different types of pile toe behaviour – namely, strain hardening and stiffening where the stiffness increases with the pile toe resistance; see Figures 10(a)–10(e) for strain hardening and Figures 11(a)–11(e) for stiffening behaviour. Table 5 summarises the proportion of strain hardening and stiffening cases.

There are approximately equal proportions of strain hardening and stiffening curves for materials where SPT N values are up to 200. For the different rock types, and except for shales, the limited data indicate that the majority exhibit strain hardening behaviour.

There are three possible reasons for the stiffening behaviour and these are listed below

(*a*) The repeated use of a cleaning bucket to clean the pile toe in materials of weathering grades III and IV may leave behind a thin layer of disturbed soil.
(*b*) Relatively open joints of highly fractured grade I, II and III rocks close up during load application.

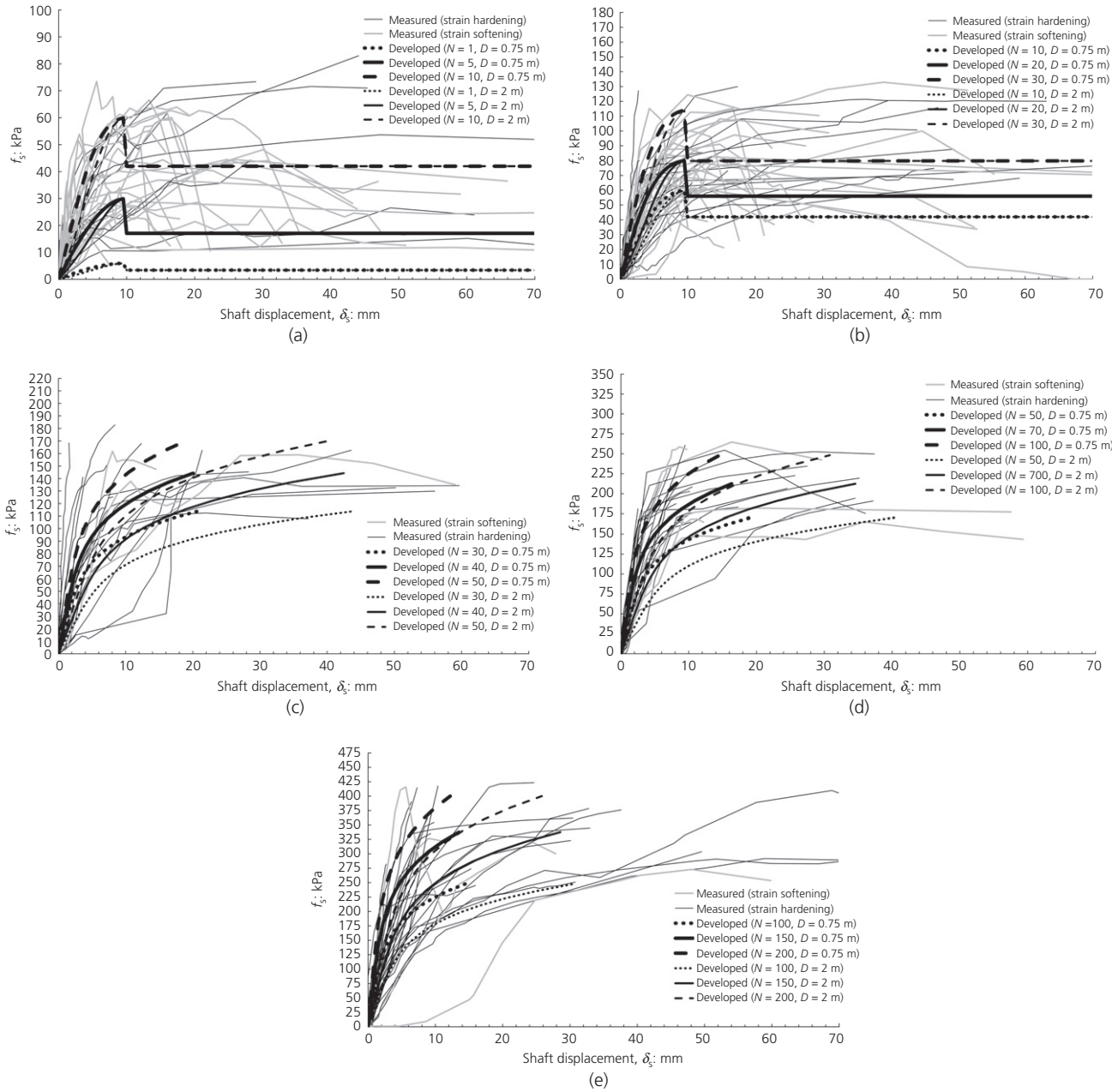

Figure 8. Measured and developed *t–z* curves for: (a) SPT $N < 10$; (b) SPT N 10 to 30; (c) SPT N 30 to 50; (d) SPT N 50 to 100; (e) SPT N 100 to 200

(*c*) The effects of orientation of joints as discussed by Kulhawy *et al*. (2005) on ultimate base capacities.

The effects of stiffening pile toe on the load–settlement behaviour of a pile will be described in Section 16.

11. Shear modulus

Unlike the shear modulus G, k_{is} is not a basic soil property and is a function of pile diameter and also pile length.

Randolph and Wroth (1978) presented the following equation relating k_{is} to G.

$$k_{is} = \frac{G}{r_0 \ln(r_m/r_0)}$$

where $r_m = 2.5\, l\,(1 - \nu)$ and l is the pile length.

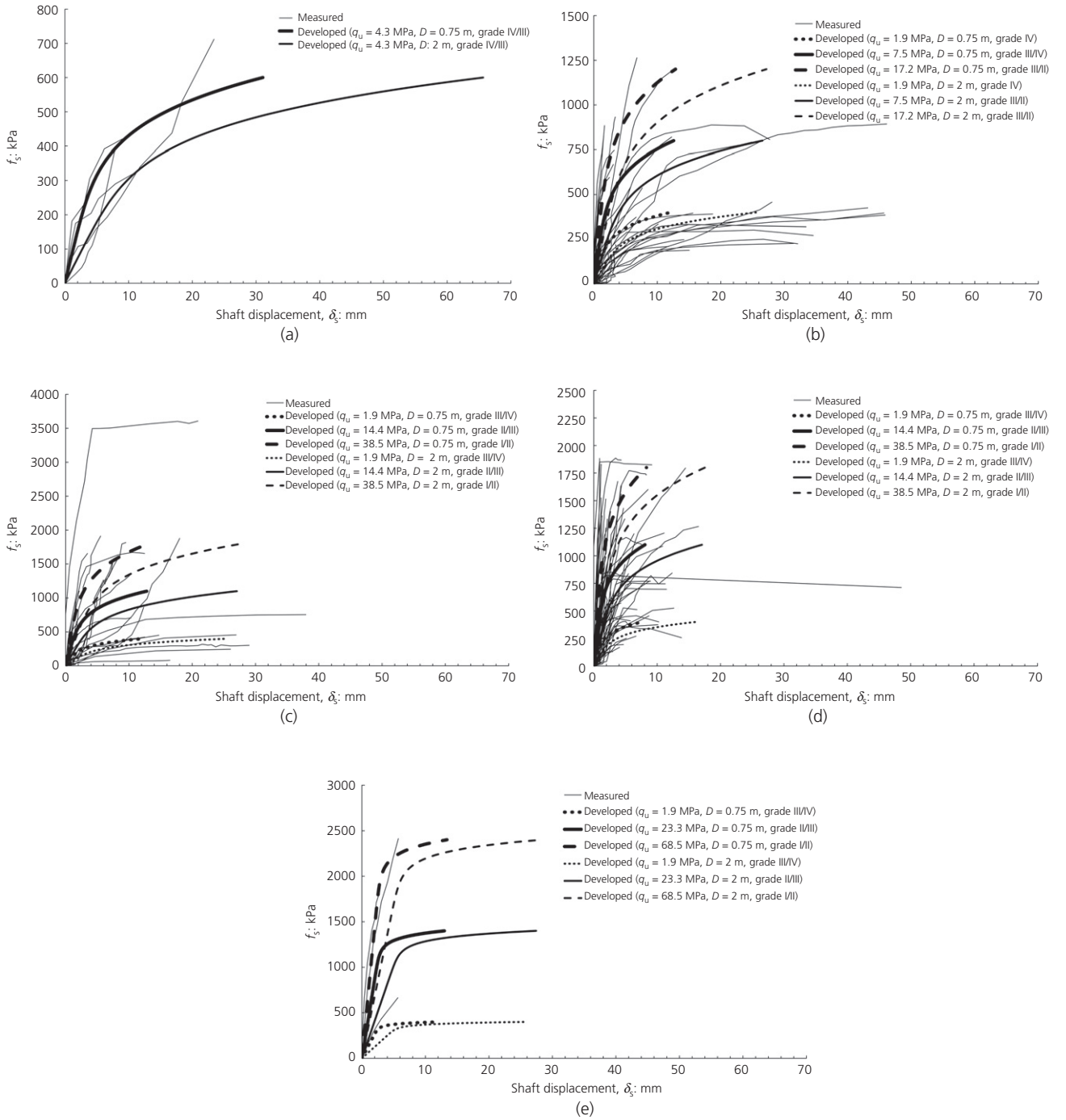

Figure 9. Measured and developed *t–z* curves for (a) shale; (b) sandstone; (c) granite; (d) limestone; (e) schist

The k_{is} values obtained from the 444 measured *t–z* curves as well as from publications were related to the shear modulus G using Randolph and Wroth's equation and the G values are plotted against q_u and N in Figure 12 assuming $C_u = 5N$. The shear modulus strength relationship may be expressed as:

$$G = AN^B$$

with $A = 0.4$, 1.6 and 6.3 for the lower bound (visually determined), mean (linear regression) and upper bound (visually determined) lines, respectively, and $B = 0.9429$ for the three conditions. The mean line is fairly similar to that by Randolph and Wroth (1978). The coefficient of determination and standard error of the mean line are 0.47 and 0.45, respectively.

Table 4. Statistics on measured strain softening and strain hardening *t–z* curves

SPT *N*	q_u: MPa	Total number of measured *t–z* curves	No. of measured strain softening *t–z* curves	No. of measured strain hardening *t–z* curves	Percentage *t–z* curves with strain softening	Percentage *t–z* curves with strain hardening
0 to 10	0 to 0.1	43	28	15	65.1	34.9
10 to 30	0.1 to 0.3	66	37	29	56.1	43.9
30 to 50	0.3 to 0.5	41	10	31	24.3	75.7
50 to 100	0.5 to 1.0	59	15	44	25.4	74.6
100 to 200	1.0 to 2.0	58	9	49	15.5	84.5
—	2.0 to 3.0	22	4	18	18.2	81.8
—	3.0 to 6.0	22	6	16	27.3	72.7
—	6.0 to 8.0	11	5	6	45.5	54.5
Total		322	114	208	35.4	64.6

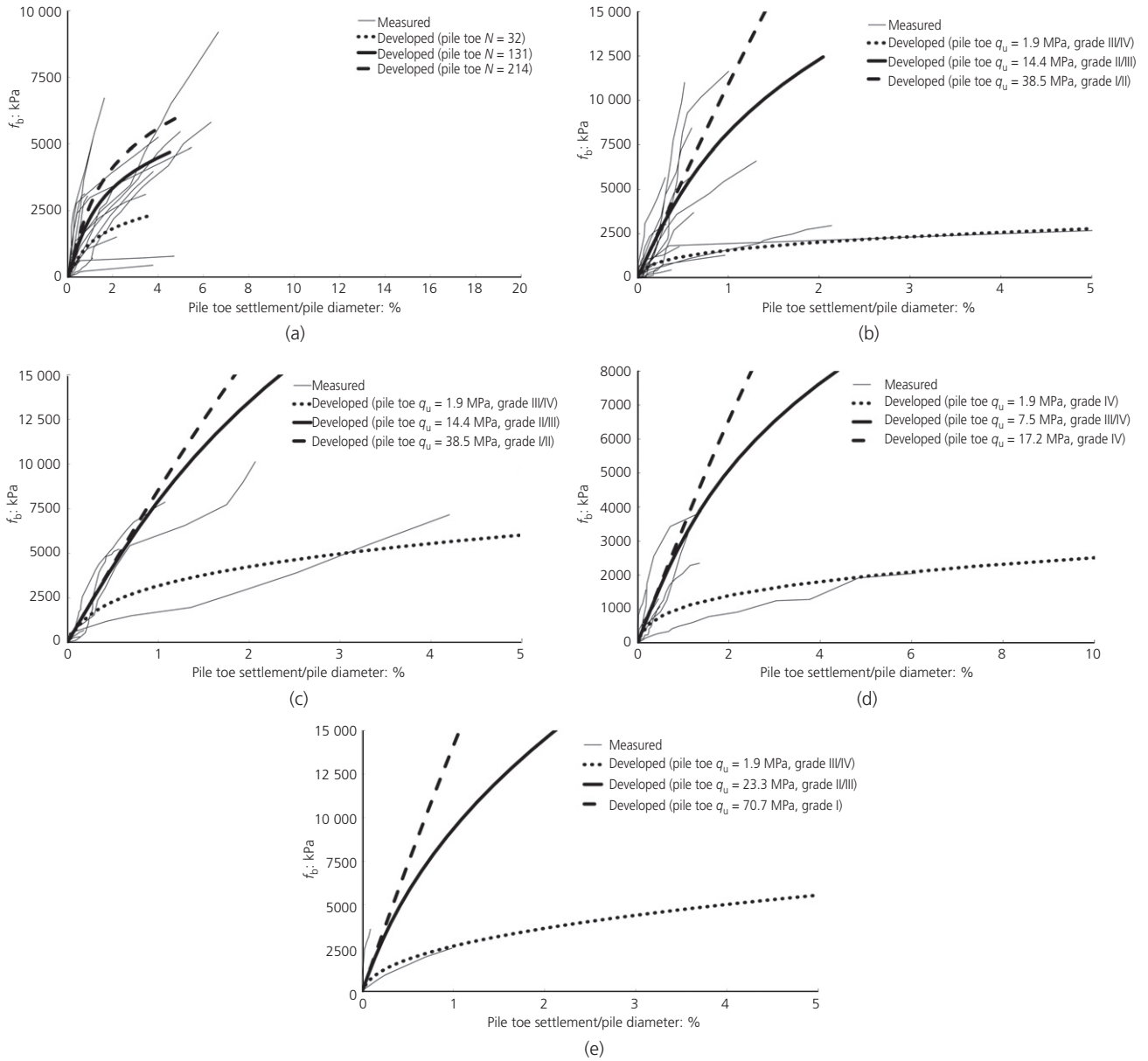

Figure 10. Measured and developed *q–w* curves: (a) strain hardening for SPT *N* up to 250; (b) strain hardening for limestone; (c) strain hardening for granite; (d) strain hardening for sandstone; (e) strain hardening for schist

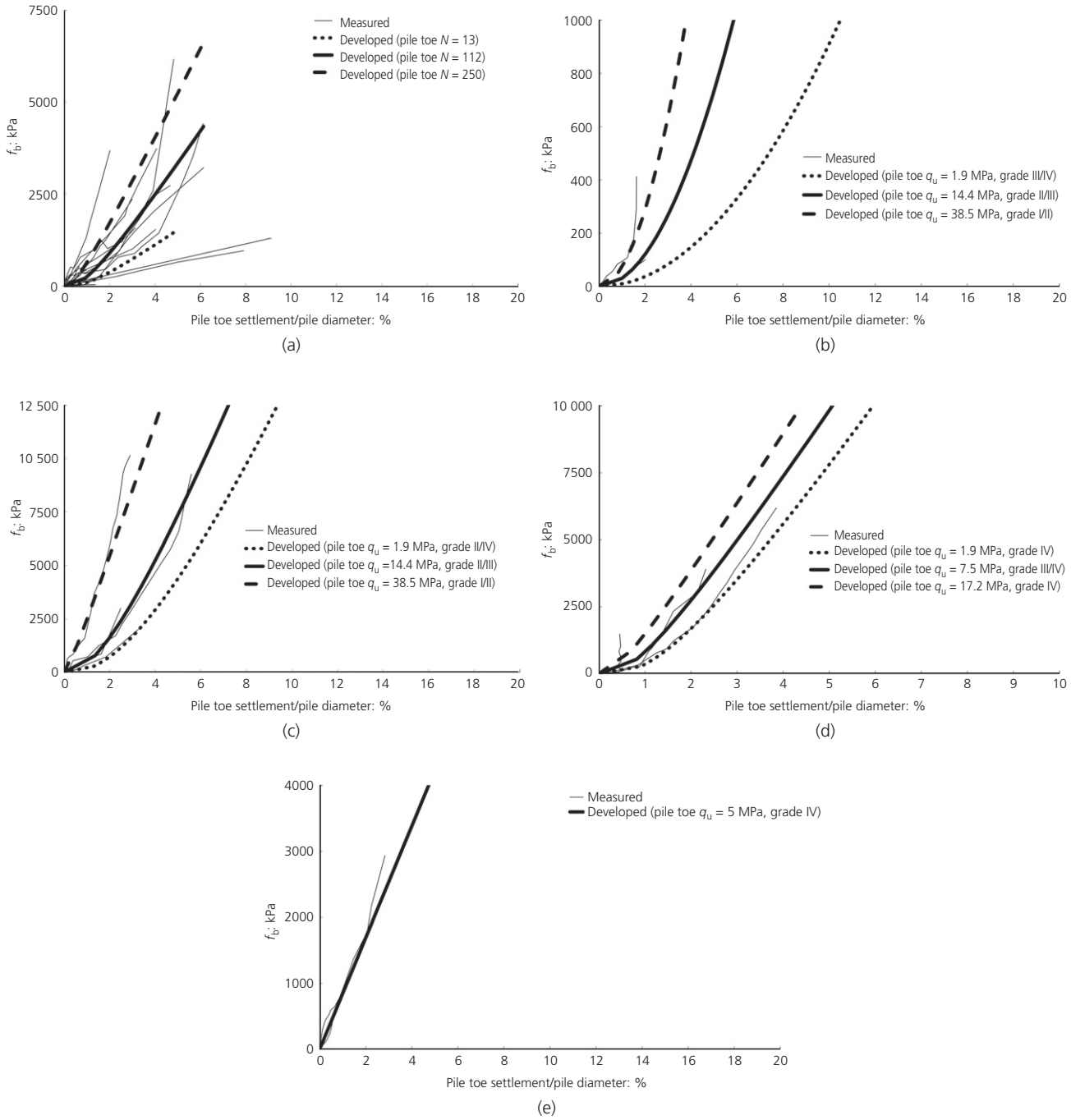

Figure 11. Measured and developed *q–w* curves: (a) stiffening for SPT *N* up to 250; (b) stiffening for limestone; (c) stiffening for granite; (d) stiffening for sandstone; (e) stiffening for shale

12. *t–z* and *q–w* functions

Bohn *et al*. (2017) summarised the various types of *t–z* functions. All the available functions are elastic–perfectly plastic; the elastic part can be linear, multi-linear or non-linear, commonly hyperbolic or root functions. There are two categories of *t–z* functions: those whose function relates to soil strength stiffness as by Frank (1984) and Randolph (2007) and those that do not. Frank (2017) related soil and rock types, pressuremeter parameters and pile types to multi-linear type *t–z* curves.

Table 5. Statistics on measured strain hardening and stiffening *q–w* curves

Description	Average SPT *N* at pile toe	Average q_u: MPa	Total number of *q–w* curves	No. of stiffening *q–w* curves	No. of strain hardening *q–w* curves	Percentage stiffening curves	Percentage strain hardening curves
Soils	131	0.131	44	24	20	55	45
Limestone	—	20	21	2	19	10	90
Granite	—	40	10	4	6	40	60
Sandstone	—	7	12	3	9	25	75
Shale	—	5	2	2	0	100	0
Schist	—	60	4	0	4	0	100
Total			93	35	58	37.6	62.4

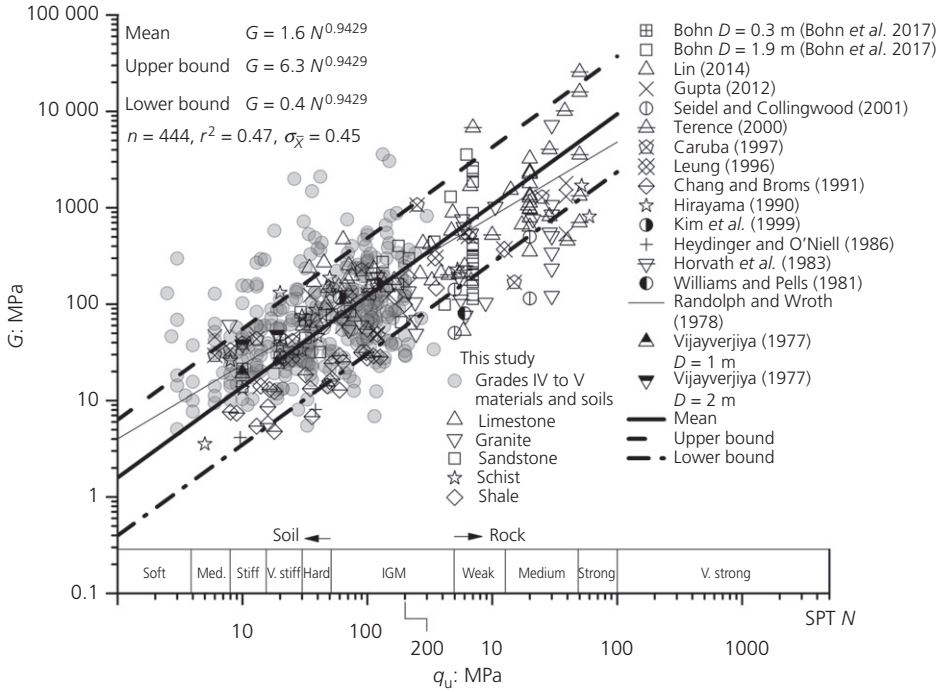

Figure 12. Back-calculated soil shear modulus plotted against q_u

In order to be able to simulate strain hardening, strain softening *t–z* curves and strain hardening and stiffening *q–w* curves, different models that were developed for structural materials were adopted and adapted for use. These were the

(*a*) Tsai (1988) function, which was developed for concrete and which can simulate non-linear pre-yield followed by perfect plasticity or strain softening
(*b*) Ramberg and Osgood (1943) function, which was developed for strain hardening alloys;

These two *t–z* functions are illustrated in Figure 13.

The Tsai equation adopted for modelling strain softening *t–z* behaviour pile is expressed as:

$$y = \frac{nx}{1 + \{n - [r/(r-1)]\}x + [x^r/(r-1)]}$$

$$x = \frac{\delta_s}{\delta_{su}}$$

$$y = \frac{f_s}{f_{su}}$$

$$n = \frac{k_{is}\delta_{su}}{f_{su}}$$

Higher r values are associated with steeper strain softening curves. The function does not place a limit on the degree of softening, but this can be imposed in the numerical scheme.

The Ramberg and Osgood model for strain hardening t–z behaviour is expressed as:

$$\delta_s = \frac{f_s}{k_{is}}\left[1 + \alpha\left(\frac{f_s}{f_{su}}\right)^{R-1}\right]$$

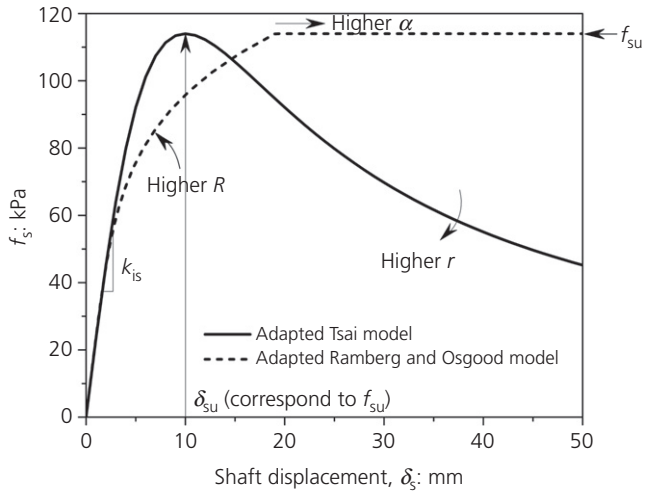

Figure 13. Adapted Tsai and Ramberg and Osgood models for t–z

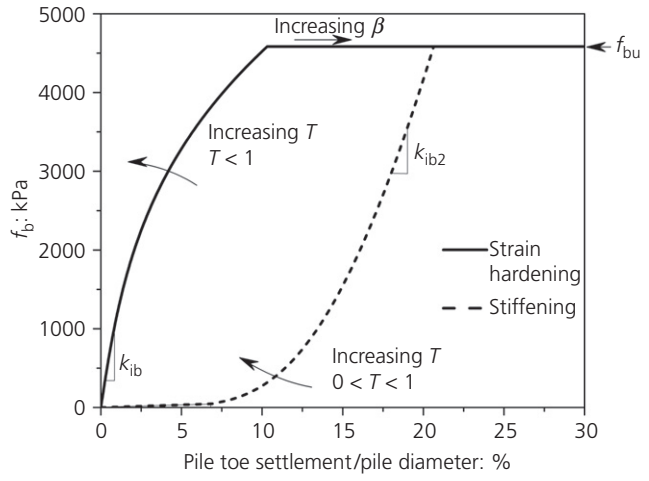

Figure 14. Adapted Ramberg and Osgood model for strain hardening and stiffening q–w

Higher R values are associated with steeper pre-yield curves. Higher α values result in higher displacements at which f_{su} is reached and the onset of perfect plastic conditions.

The Ramberg and Osgood model for strain hardening and stiffening q–w behaviour is illustrated in Figure 14 and expressed as:

$$\delta_b = \frac{f_b}{k_{ib}}\left[1 + \beta\left(\frac{f_b}{f_{bu}}\right)^{T-1}\right]$$

where $T > 1$ for strain hardening and

$$\delta_b = \frac{f_b}{k_{ib2}}\left[1 + \beta\left(\frac{f_b}{f_{bu}}\right)^{T-1}\right]$$

where $0 < T < 1$ for stiffening.

13. Developing *t–z* models

13.1 Tsai model for strain softening

For materials up to SPT N of 200, it is recommended that f_{su} be obtained from the median line of Figure 1. For harder materials, α_q is best obtained from the mean line of Figure 4.

G values should be obtained from the mean equation of Figure 12. k_{is} is computed from G using the Randolph and Wroth (1978) equation.

The other parameters required for the Tsai model are δ_{su} and r. For these, statistical analyses of 29 t–z curves for SPT N less than 10 and another 39 curves for SPT N between 10 and 30 were carried out. The results are presented in Tables 6 and 7 for δ_{su} and r, respectively. The significant variations shown in Figures 8(a) and 8(b) are reflected in the large standard deviations (SDs). Such scatter is not unexpected considering the different types of geological formations and the material differences. In the light of the significant scatter and for want of a better approach, it is proposed that the median values be

Table 6. Statistics for δ_{su} (Tsai's t–z model)

SPT N	No. of samples	Mean	Median	SD
$N < 10$	29	12.92	11.25	8.29
$10 \le N < 30$	39	13.36	11.00	9.38

Table 7. Statistics for r (Tsai's t–z model)

SPT N	No. of samples	Mean	Median	SD
$N < 10$	29	6.46	4.00	6.38
$10 \le N < 30$	39	3.83	2.00	4.79
$30 \le N < 50$	12	4.08	1.40	7.15

Table 8. Statistics for α (Ramberg and Osgood's *t–z* model)

SPT *N*	No. of samples	Mean	Median	SD
$30 \leq N < 50$	34	6.72	2.55	8.06
$50 \leq N < 100$	47	7.16	2.95	11.60
$100 \leq N < 200$	49	8.06	3.50	12.34

Table 9. Statistics for *R* (Ramberg and Osgood's *t–z* model)

SPT *N*	No. of samples	Mean	Median	SD
$30 \leq N < 50$	34	8.83	5.00	9.45
$50 \leq N < 100$	47	6.83	5.00	4.26
$100 \leq N < 200$	49	5.67	5.00	3.67

adopted. The final test of this choice is whether the *t–z* curves can be used to estimate reasonably accurately the performance of a pile.

13.2 Ramberg and Osgood model for strain hardening

The recommended method for obtaining f_{su} and α_q is the same as described in Section 13.1.

The other parameters required to define the model are α and *R*. A total of 130 *t–z* curves for the range of SPT *N* from 30 to 200 were subdivided into three different SPT groups for statistical analysis. The results are presented in Tables 8 and 9 for α and *R*, respectively.

Again there is significant variation in the *t–z* curves, which is reflected in the high SDs. Again the median values that

Table 10. Proposed parameters for *t–z* models for grade III to VI and soils related to SPT *N*

SPT *N*	Approximate weathering or decomposition grade	f_{su}: kPa (Figure 1 median line)	k_{is}: kPa/mm (from mean *G* equation of Figure 12)		Tsai model for strain softening		Ramberg and Osgood model for strain hardening	
			Diameter 0.75 m	Diameter 2 m	δ_{su}: mm	*r*	α	*R*
1	Soils and VI	6	1.2	0.6	10.0	4.0	—	—
5		30	5.3	2.7	10.0	4.0	—	—
10		60	13.9	5.3	10.0	4.0	—	—
20		80	19.7	10.1	10.0	2.0	—	—
30		114	23.9	11.5	10.0	2.0	—	—
40	V	144	31.3	15.1	—	—	3.0	5.0
50		171	35.5	16.8	—	—	3.0	5.0
75		213	52.0	24.5	—	—	3.0	5.0
100	IV/V	248	68.3	32.2	—	—	3.0	5.0
150		338	100.0	47.3	—	—	3.0	5.0
200	III/IV	400	131.2	62.0	—	—	3.0	5.0

Table 11. Proposed parameters for *t–z* model for rock types and related strengths

Rock type	Approximate weathering or decomposition grade	q_u: MPa	f_{su}: kPa (Figure 4 mean)	k_{is}: kPa/mm			Ramberg and Osgood model	
				Diameter 0.75 m	Diameter 2 m	Recommended values for all pile sizes	α	*R*
Shale	III/IV	4.3	600	77.3	36.6	50	3.0	5.0
Sandstone	IV	1.9	400	132.4	62.7	56	3.0	5.0
	III/IV	7.5	800	254.5	120.0	112		
	II/III	17.2	1200	373.0	176.6	168		
Granite	III/IV	1.9	400	132.4	62.7	90	3.0	5.0
	II/III	14.4	1100	343.6	162.7	247		
	I/II	38.5	1800	546.7	258.8	404		
Limestone	III/IV	1.9	400	209.8	99.3	118	3.0	5.0
	II/III	14.4	1100	544.6	257.8	324		
	I/II	38.5	1800	866.4	410.2	531		
Schist	III/IV	1.9	400	132.4	62.7	150	3.0	20.0
	II/III	23.3	1400	431.3	204.2	375		
	I/II	68.5	2400	717.0	339.4	600		

happen to be similar for the different SPT N groups are proposed for the model.

13.3 Proposed parameters and developed *t–z* curves

A summary of the proposed parameters for the Tsai and Ramberg and Osgood *t–z* models is given in Table 10 for soils and grade IV to V materials with related SPT N values and Table 11 for different rock types and range of weathering grades. The k_{is} values are for 750 mm and 2000 mm diameter piles.

The resulting developed *t–z* curves are plotted against the measured *t–z* curves in Figures 8(a)–8(e) and 9(a)–9(e).

A comparison of the developed *t–z* curves for different SPT N values up to 200 for pile diameters of 750 mm and 2000 mm is shown in Figure 15(a). The difference in the *t–z* curves for 750 mm and 2000 mm piles becomes apparent for larger SPT N values. Figure 15(b) shows *t–z* curves for the different rock types also for 750 mm and 2000 mm diameter piles. The *t–z* curves for piles of larger diameter are softer, but the percentage differences for the two pile sizes are lower for the lower strength rocks. It was found from analysis of the piles (see Sections 16 and 17) that improved estimates of the load–settlement curves can be made by using the recommended k_{is} parameters given in Table 11; these recommended k_{is} values are independent of pile sizes.

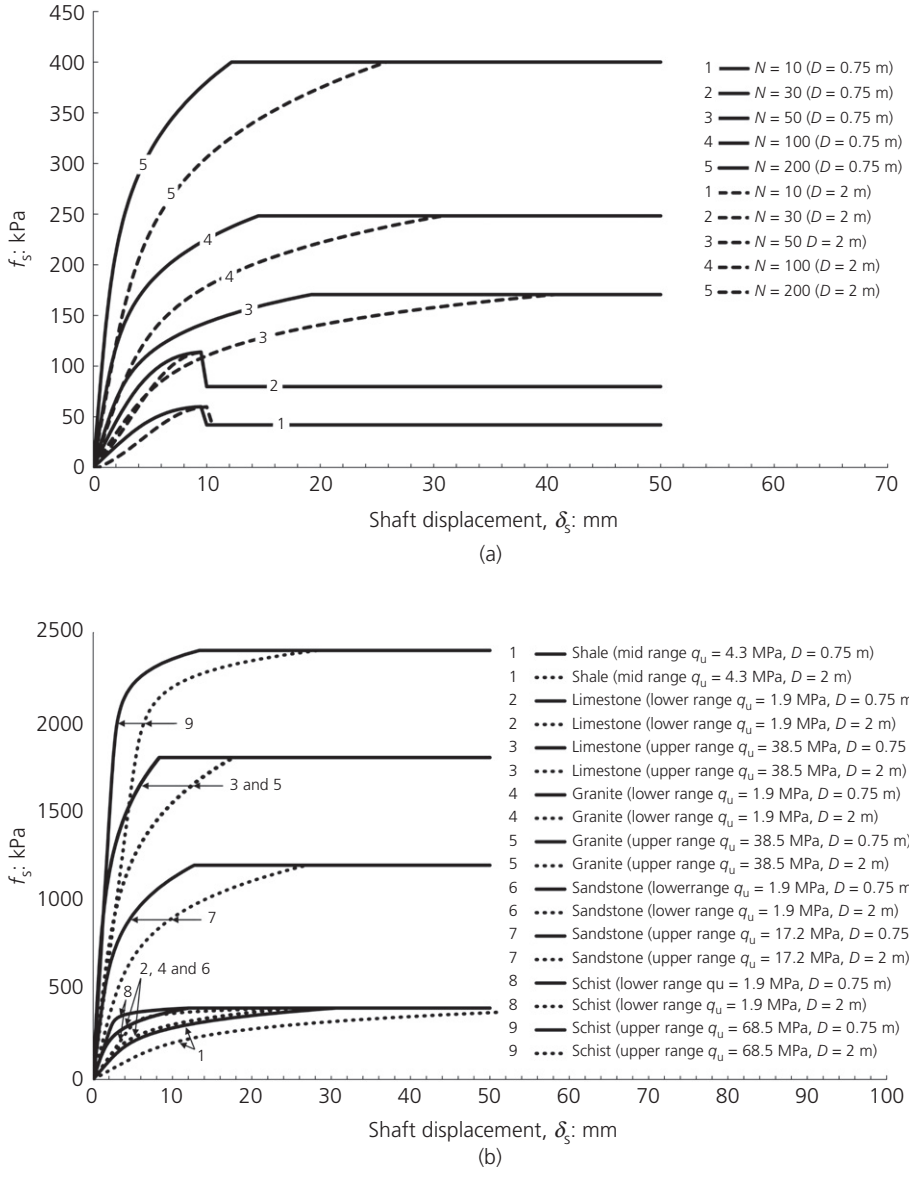

Figure 15. Developed *t–z* curves: (a) for SPT N up to 200; (b) for different rock types

14. Developing *q–w* models

The k_{ib} values obtained from the 51 measured strain hardening q–w curves and k_{ib2} from the 25 measured stiffening curves are plotted against SPT N and q_u in Figure 16. k_{ib} and k_{ib2} can be obtained from q_u or SPT N by use of the mean equation given in Figure 16. There is considerable scatter with the following expressions for the mean:

$$k_{ib} = 2329.6q_u^{0.3493} \quad \text{for strain hardening}$$

$$k_{ib2} = 951.15q_u^{0.3292} \quad \text{for stiffening}$$

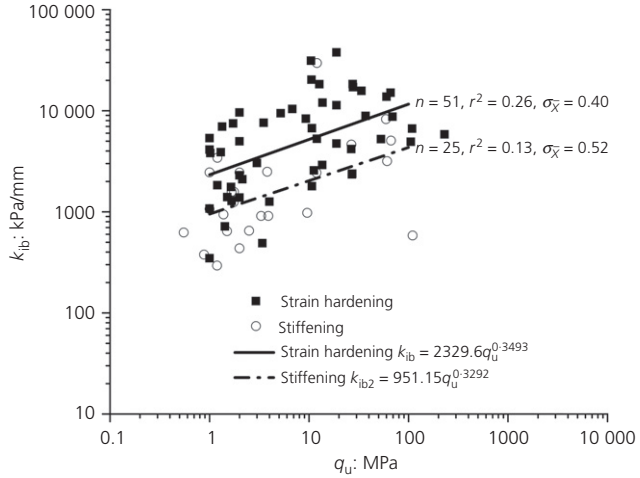

Figure 16. Measured K_{ib} and K_{ib2} plotted against q_u

Table 12. Statistics for k_{ib} (Ramberg and Osgood's strain hardening q–w model)

	No. of samples	k_{ib} (from mean k_{ib} equation of Figure 16)		
		Mean	Median	SD
Limestone	19	11 155	8886	8704
Granite	6	8757	8262	5280
Sandstone	9	3437	3039	9496
Schist	1	4174	4174	0

The other parameters for defining a strain hardening q–w curve are T and β. Statistical analyses from curve fitting the q–w curves are summarised in Table 12 for k_{ib} and Table 13 for β and T. As is apparent from Figure 16, the scatter is significant and SDs are high. The coefficient of determination and standard error for the mean line are 0.26 and 0.40, respectively, whereas for k_{ib2} the coefficient of determination and standard error are 0.13 and 0.52, respectively. Median values are proposed for use.

Tables 14 and 15 are the results of statistical analysis of k_{ib2}, β and T for stiffening curves. Again the scatter is large and median values are proposed for use. The proposed parameters for strain hardening and stiffening q–w curves are given in Tables 16 and 17 for a range of rock types and weathering grades. The q–w curves developed from the parameters in Tables 16 and 17 are shown in Figures 17(a) and 17(b). Stiffening curves do not follow rock strengths, as many other factors such as pile toe cleanliness, joint conditions, their orientations and spacing and deterioration of shales on exposure influence the behaviour.

15. Method for estimating pile behaviour

The procedure for estimating the performance of a pile is as follows.

Soil profile

(*a*) Divide the sub-surface into layers, each with a representative SPT N or q_u.

t–z curves

(*a*) For each layer obtain median K_s from Figure 1 or mean α_q from Figure 4.
(*b*) Obtain an estimate of shear modulus from the mean equation in Figure 12.
(*c*) Estimate k_{is} using Randolph and Wroth equation.

Table 13. Statistics for β and T (Ramberg and Osgood's strain hardening q–w model)

	No. of samples	β			T		
		Mean	Median	SD	Mean	Median	SD
Soils	12	3.90	1.46	6.94	4.30	4.00	1.73
Limestone	5	8.18	1.30	15.01	3.90	3.00	2.13
Granite	4	1.33	1.05	0.88	4.13	3.00	2.59
Sandstone	5	1.58	1.60	1.18	4.80	3.00	2.95
Schist	2	1.60	1.60	1.38	3.25	3.30	1.06

Table 14. Statistics for k_{ib2} (Ramberg and Osgood's stiffening model)

	No. of samples	k_{ib2} (from mean k_{ib2} equation of Figure 16)		
		Mean	Median	SD
Limestone	1	8285	8285	0
Granite	4	3586	2415	3947
Sandstone	2	2807	2807	522
Schist	2	509	509	104
Shale	2	845	845	47

(*d*) For SPT N less than 30, adopt the strain softening model and develop the t–z curve using the Tsai model with parameters from Table 10. Introduce a limit to the strain softening.

(*e*) For SPT N greater than 30, adopt the strain hardening model and develop the t–z curve using the Ramberg and Osgood model with the recommended parameters in Tables 10 and 11.

Table 15. Statistics for β and T (Ramberg and Osgood's stiffening q–w model)

	No. of samples	β			T		
		Mean	Median	SD	Mean	Median	SD
Soils	13	0.64	0.66	0.43	0.31	0.30	0.14
Limestone	1	31.50	31.50	—	0.50	0.50	—
Granite	4	0.96	0.78	0.62	0.38	0.40	0.05
Sandstone	3	0.80	0.80	0.28	0.23	0.30	0.12

Table 16. Proposed parameters for strain hardening q–w Ramberg and Osgood's model

Description	Approximate weathering or decomposition grade	SPT N at pile toe	q_u: MPa	f_{bu}: kPa	Strain hardening parameters		
					k_{ib}	β	T
Soils	VI	32	0.32	2319	2329.6 $N^{0.3493}$	1.46	4.0
All rock types	IV/V	131	1.31	4692			
	III/IV	214	2.14	5998			
Limestone	III/ IV	—	1.90	5651	11 155	1.30	3.0
	II/III	—	14.40	15 558			
	I/II	—	38.50	25 440			
Granite	III/IV	—	1.90	5651	8757	1.05	3.0
	II/III	—	14.40	15 558			
	I/II	—	38.50	25 440			
Sandstone	IV	—	1.90	5651	3437	1.60	3.0
	III/IV	—	7.50	11 228			
	IV	—	17.20	17 004			
Schist	III/IV	—	1.90	5651	15 000	1.60	3.3
	II/III	—	23.30	19 791			
	I/II	—	70.70	34 474			

Table 17. Proposed parameters for stiffening q–w Ramberg and Osgood's model

Description	Approximate weathering or decomposition grade	SPT N at pile toe	q_u: MPa	f_{bmax}: kPa	Stiffening parameters		
					k_{ib2}	β	T
Soils	VI	13	0.13	1478	951.15SPT $N^{0.3292}$	0.66	0.3
All rock types	VI/V	112	1.12	4339			
	III/IV	250	2.50	6483			
Limestone	III/IV	—	1.90	5651	8285	31.50	0.5
	II/III	—	14.40	15 558			
	I/II	—	38.50	25 440			
Granite	III/IV	—	1.90	5651	3274	0.78	0.4
	II/III	—	14.40	15 558			
	I/II	—	38.50	25 440			
Sandstone	IV	—	1.90	5651	2807	0.80	0.3
	III/IV	—	7.50	11 228			
	IV	—	17.20	17 004			
Shale	III/IV	—	5.00	9168	845	—	—

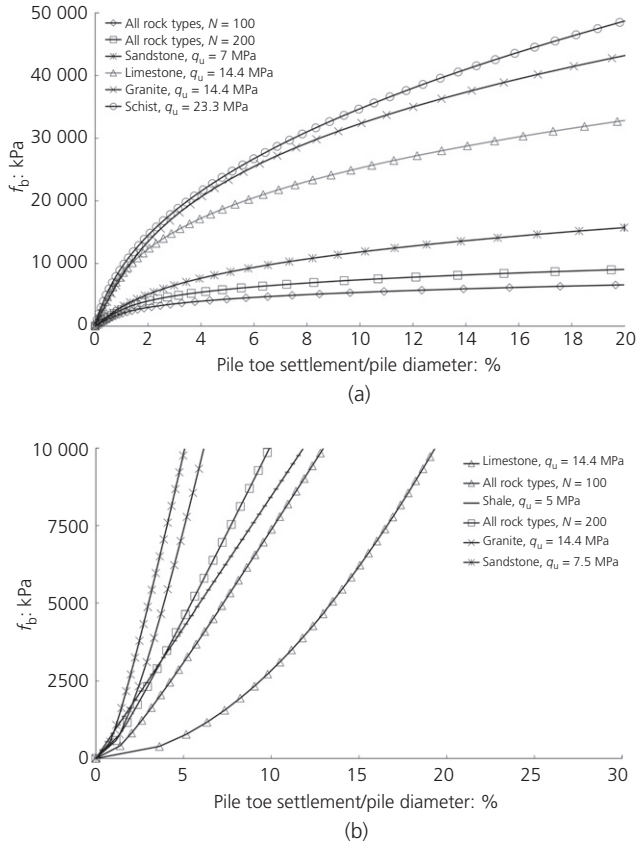

Figure 17. (a) Developed strain hardening *q–w* curves. (b) Developed stiffening *q–w* curves

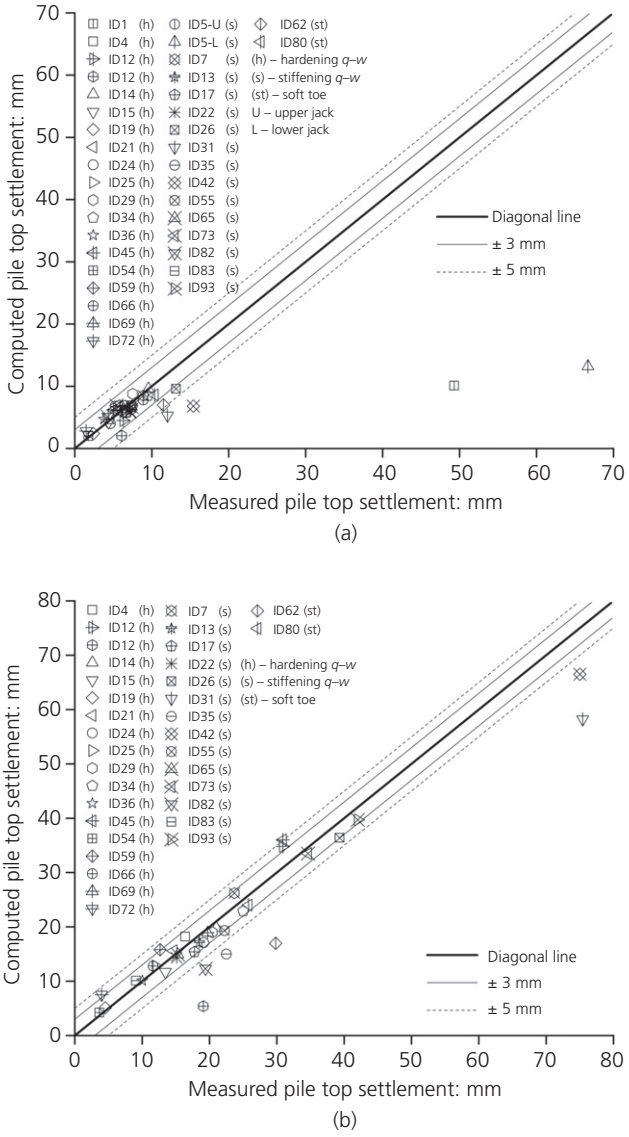

Figure 18. (a) Computed and measured pile top settlement at working load for 35 piles within database. (b) Computed and measured pile top settlement at 2×working load for 35 piles within database

q–w curves

(*a*) Decide on the likelihood of strain hardening or stiffening. This depends on the confidence in cleaning the pile toe, rock type and whether rock is highly fractured with open joints.
(*b*) Determine f_{bu} from Figure 7 using $A = 4.1$.
(*c*) Obtain an estimate of k_{ib} (strain hardening), k_{ib2} (stiffening) from the mean equation in Figure 16.
(*d*) Develop the Ramberg and Osgood *q–w* model using the parameters given in Table 16 for strain hardening and Table 17 for stiffening.

Input the developed *t–z* and *q–w* curves for the different layers into a program for *t–z* analysis of piles.

16. Estimating pile behaviour and comparing with some of the instrumented test piles' results

The models with the parameters derived above are used to estimate the pile top load–settlement response of 35 of the 100 instrumented piles of the database to test the degree of model reliability. One problem in the analysis is the need to decide a priori between strain hardening and stiffening pile toe behaviour. In the calculations for the 35 piles, the *q–w* model from the known pile toe behaviour, as shown in the instrumented test pile results, was adopted. The results of the analysis are shown in Figures 18(a) and 18(b). For most cases, the comparison between calculated and measured, including highly non-linear load–settlement behaviour, is encouraging, with most of the estimated settlements at working load and at twice working load within 3 mm and 5 mm of the actual, respectively.

Table 18. Detailed analysis of piles from the database

Case	Geology	Pile diameter: mm	Pile length: m	WL: kN	Max. load	Measured, *q–w*	Comparison of pile top load–settlement curve		Difference in load-settlement between hardening and stiffening	Comparison of load-transfer curves with measured
							Strain hardening	Stiffening		
A	Sedimentary	750	50.6	3300	3WL	Hardening	Good match with measured up to 3WL	Good match with actual up to 3WL	Little difference because the hardening and stiffening *q–w* curves similar	Good match at WL and 2WL. Appreciable difference at 3WL
B	Socketed in highly fractured limestone	1500	38.0	15 460	2WL	Hardening	Good match with measured up to 2WL	Good match with measured up to 2WL	Differ significantly after 2WL due to higher base load after 2WL	Good match at WL at 2WL
C	Sedimentary	900	16.0	5550	2.5WL	Hardening	Good match with measured up to 2.5WL	Good match with measured up to 1.7 WL	Differ significantly after 1.7WL due to higher base load after 1.7WL	Good match at WL and 2WL. Appreciable difference at 2.5WL
D	Granite	900	29.8	5550	2.5WL	Stiffening	Good match with measured up to 1.5WL	Good match with measured up to 2.5 WL	Differ significantly after 1.7WL due to higher base load after 1.7WL	Reasonable match at WL, 2WL and 2.5WL
E	Sedimentary	1000	34.0	5890	2.5WL	Stiffening	Good match with measured up to 1.5WL	Good match with measured up to 2.5 WL	Differ significantly after 1.5WL due to higher base load after 1.5WL	Good match at WL, 2WL and 2.5WL
F	Shale	900	25.8	5500	3WL	Stiffening	Good match with measured up to 3WL		Not applicable	Good match at WL, 2WL and 3WL

The two piles that showed significant differences between the estimated and actual settlement are piles ID1 and ID5. Pile ID1 is located at the junction of limestone and Kenny Hill (sedimentary) formation. The sub-surface conditions at interfaces between the two different geological formations are complex. The back-calculated K_s values are 2, corresponding to the lower bound conditions compared to the median value of 4. Pile ID5 is a bi-directional load test. For the pile length above the load cell, the difference between measured and actual movement is 1 mm. However, for the length below the load cell, the difference is 54 mm. It is thought that this may be due to poor concrete in contact with the lower plate of the bi-directional load cell.

The detailed results of the analyses for six of the 35 piles are described in Table 18 and are shown in Figures 19–24. For all six cases, strain hardening as well as stiffening *q–w* models were used. The estimated load–settlement curves were found to compare well with the measured ones up to 2.5 to 3 times the working load when the behaviour was significantly non-linear provided the correct type of *q–w* curve was adopted. If in the event the *q–w* type is not that measured, it was found that a reasonably good match with measured was achieved up to about 1.5 to 2 times working load before significant mobilisation of base resistance resulted in larger differences. The proposed *t–z* curve for the different strengths and geological formations are always between the lower and upper bound lines (see Figures 8 and 9). Therefore, it may be expected that often there will be differences between the *t–z* models and the actual *t–z* curves resulting in variations from the actual load-transfer curves. A difference in axial load at depth of up to 54% was estimated for case A (Figure 19). However, for case B (Figure 20) to case F (Figure 24), the maximum difference in the axial load at depth was found to be less than 19%.

17. Estimating pile behaviour and comparing with pile tests outside the database

The results of 27 test piles with comprehensive sub-surface information, SPT N or q_u profiles, were obtained from the available literature and used for testing the proposed models. The 27 piles were from across the globe and include a few piles outside the tropics. A description of the piles is given in Appendix 2. Figures 25(a) and 25(b) illustrate the comparisons of the settlement at maximum test load and at half the maximum test load. At half the maximum test load, most of the estimates of settlement differ from the actual by less than 3 mm, whereas at maximum test load, most of the estimated settlements differ from the actual by not more than 5 mm. Figures 26(a) and 26(b) compare the estimated and actual load settlement curves for seven cases.

There was greater difference between the estimated and actual pile behaviour for three out of 27 piles; one in chalk (UK), one in shale (Taiwan) and one in alluvial sand (Japan). For the

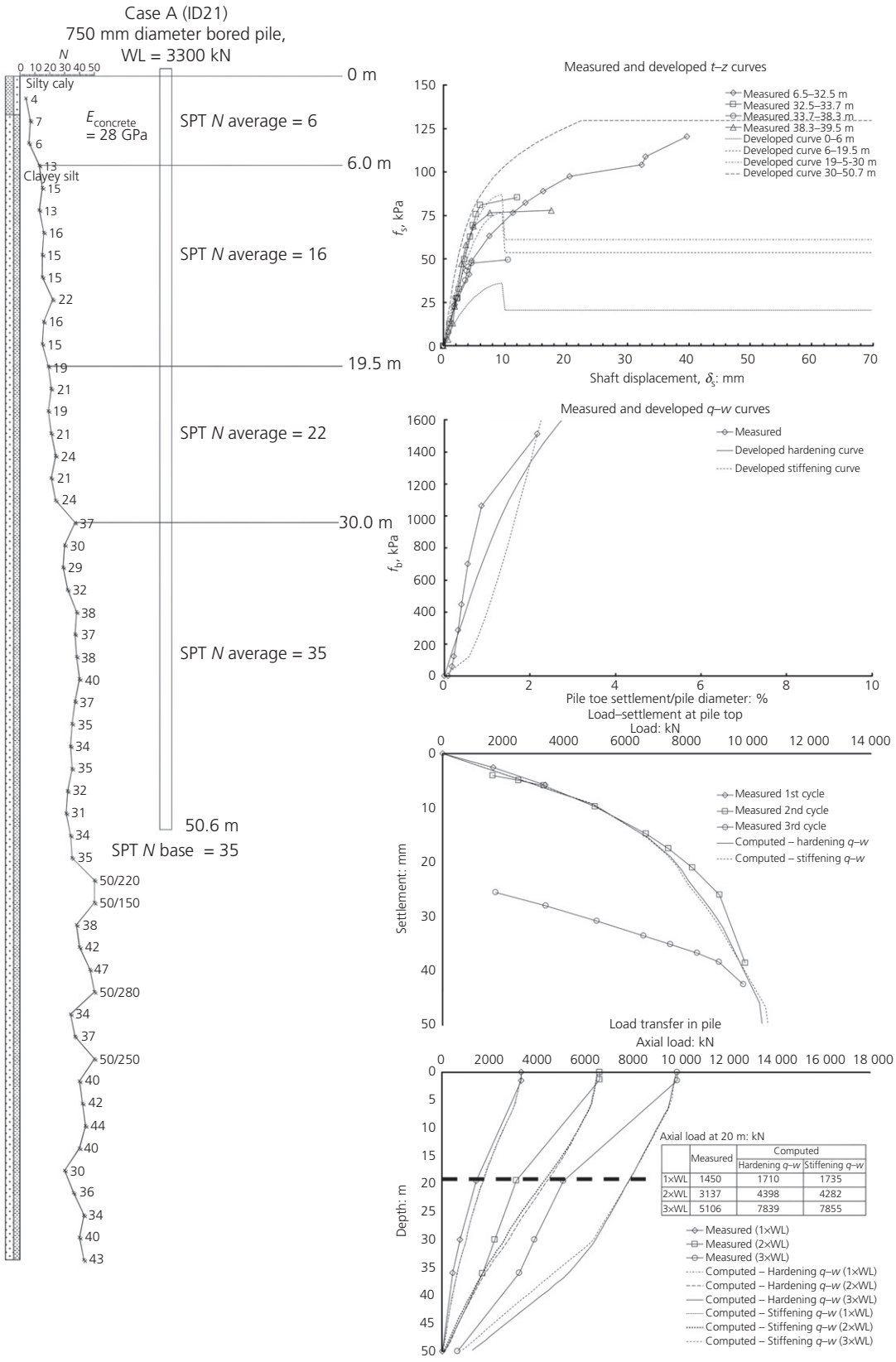

Figure 19. Application of proposed *t–z* and *q–w* – case A

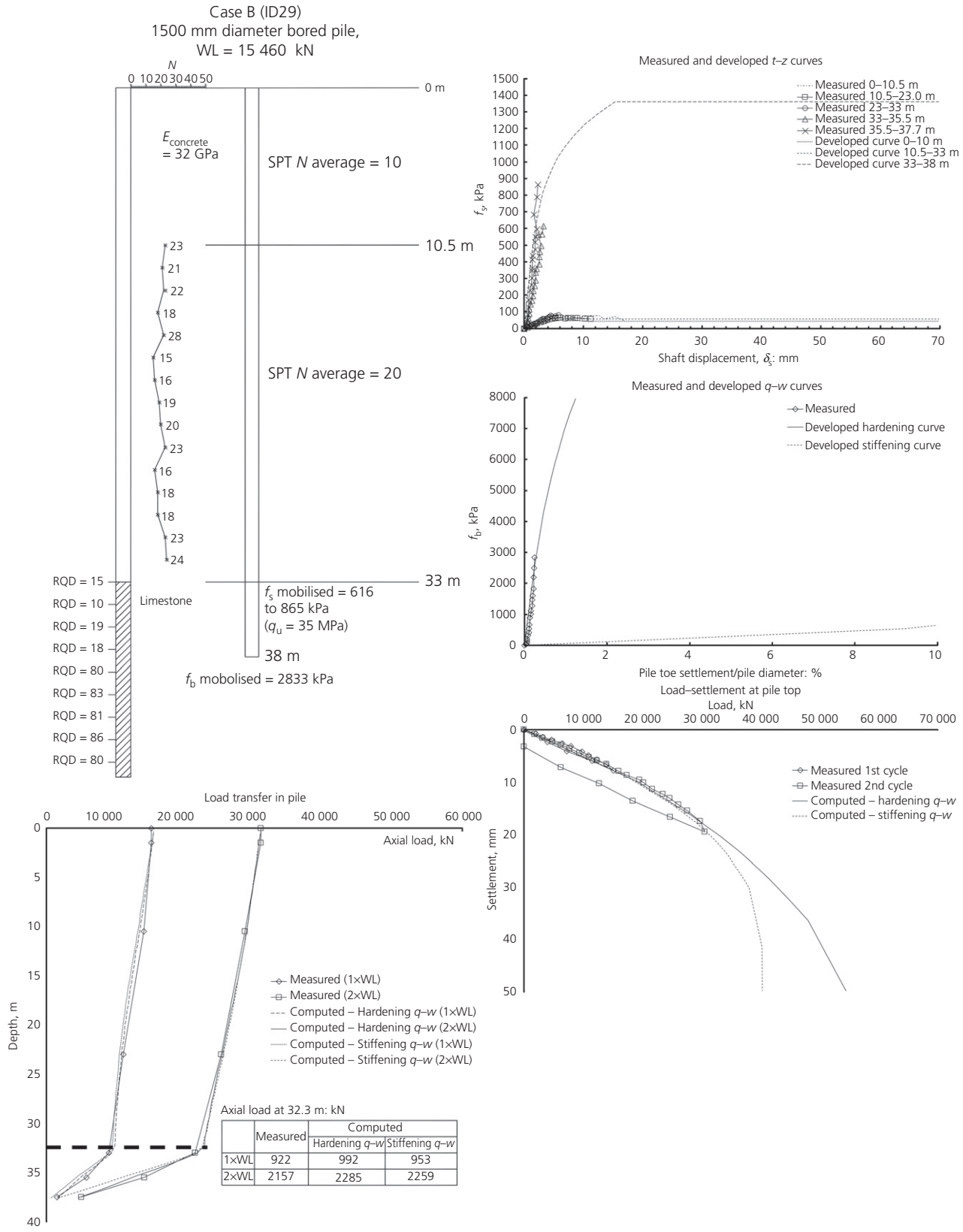

	Measured	Computed	
		Hardening *q–w*	Stiffening *q–w*
1×WL	922	992	953
2×WL	2157	2285	2259

Figure 20. Application of proposed *t–z* and *q–w* – case B

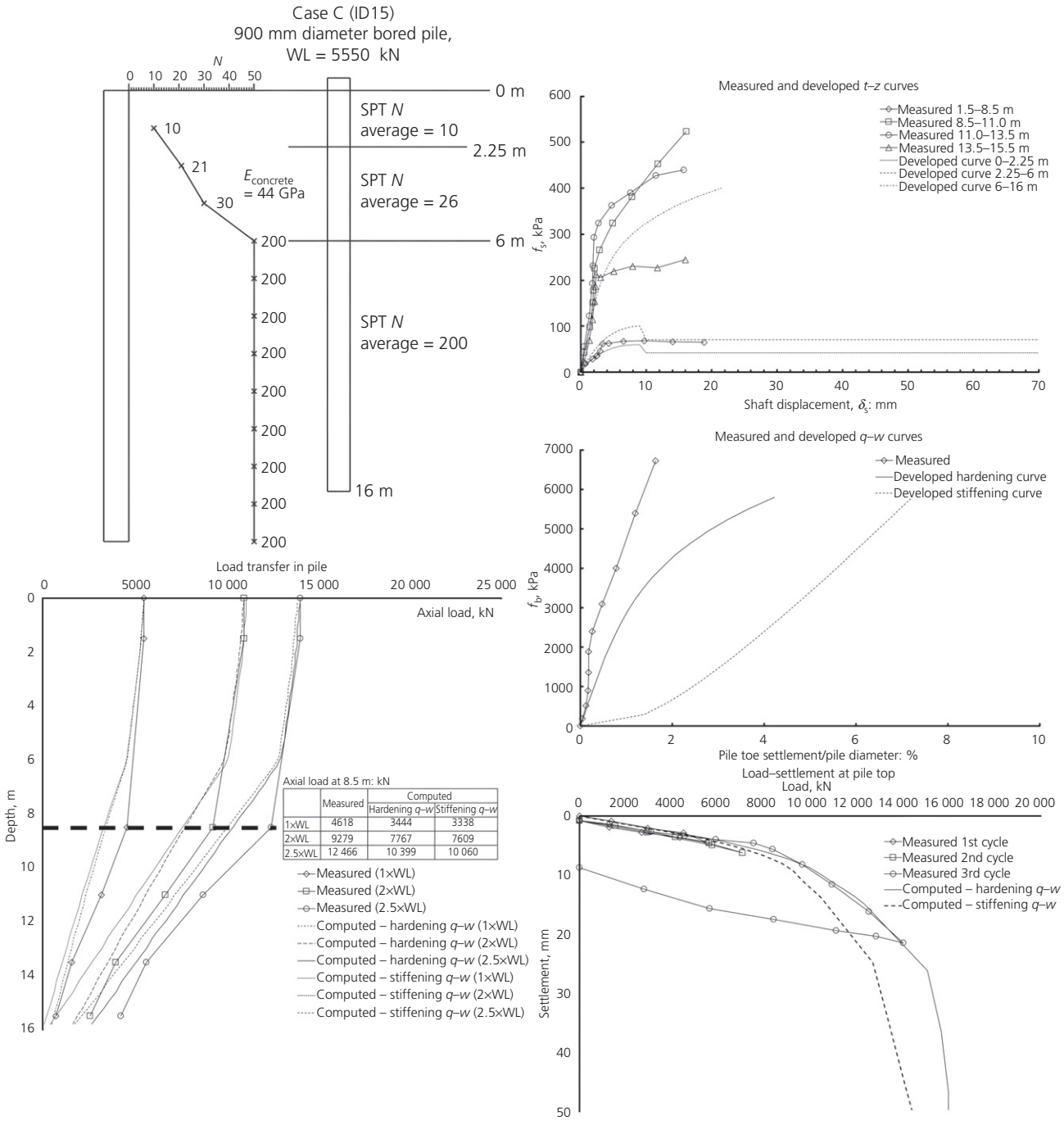

Figure 21. Application of proposed *t–z* and *q–w* – case C

three piles the difference in settlements between estimated and actual at half the maximum test load and at maximum test load were 10 mm and 20 mm, respectively. The inability to make a better estimate for these three piles is largely because the correlations between f_{su}, f_{bu} and G with strength are different from the tropical soils in this paper.

18. Summary and conclusions

(*a*) Data from 100 instrumented test piles that extend over the complete weathering profiles of different geological formations were analysed to provide ultimate shaft and base parameters.

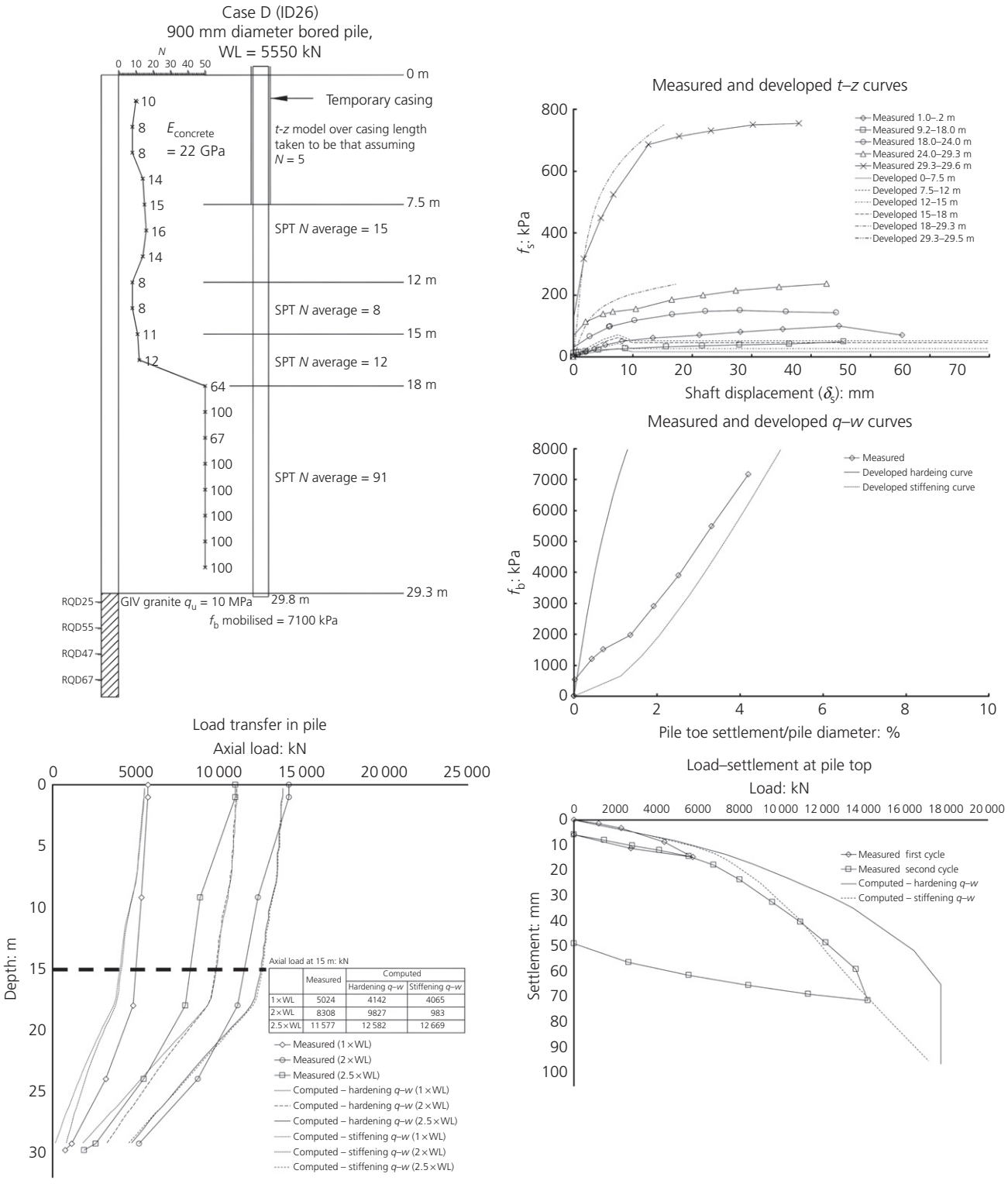

	Measured	Computed	
		Hardening *q–w*	Stiffening *q–w*
1×WL	5024	4142	4065
2×WL	8308	9827	983
2.5×WL	11 577	12 582	12 669

Figure 22. Application of proposed *t–z* and *q–w* – case D

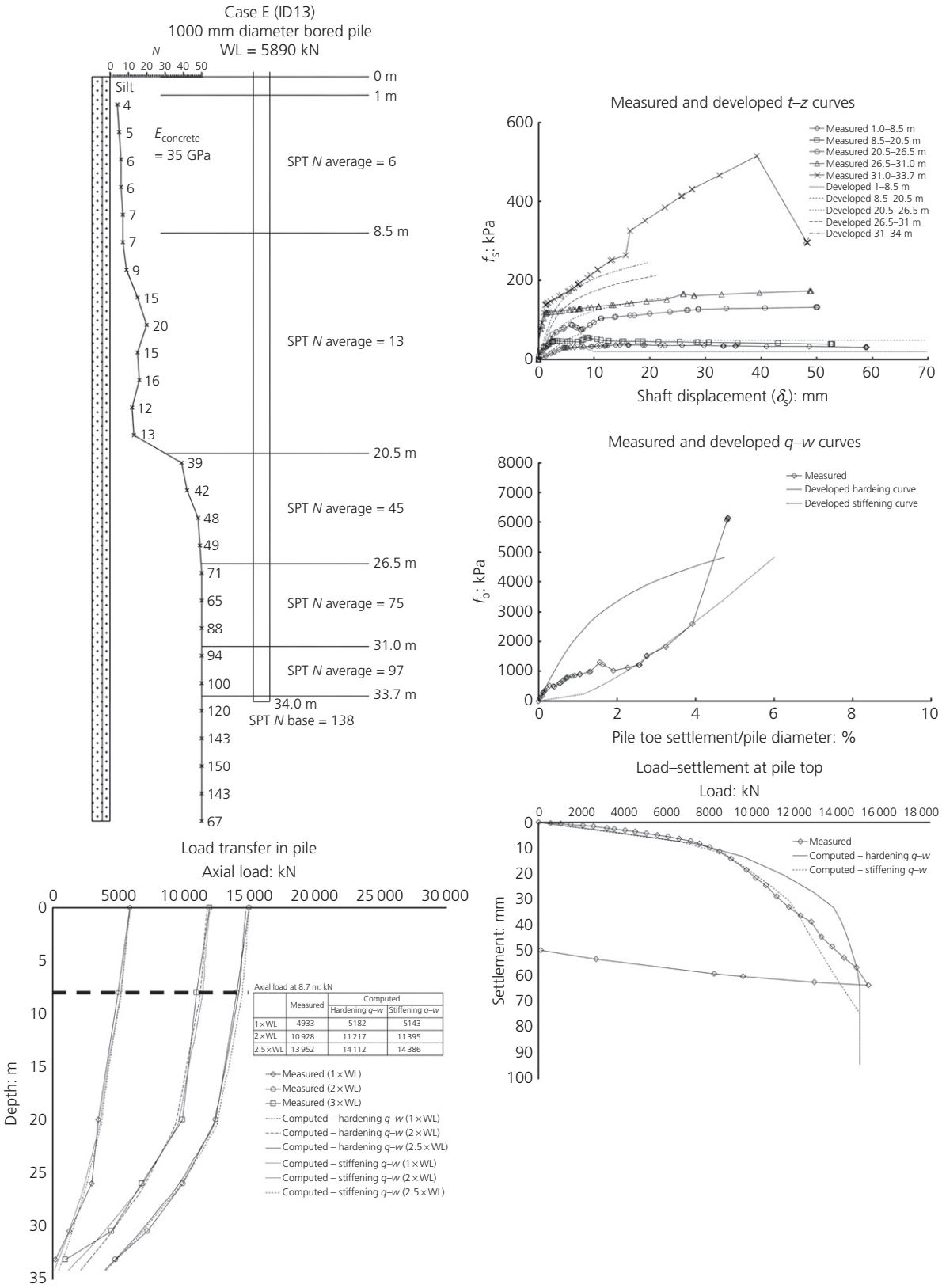

Figure 23. Application of proposed *t–z* and *q–w* – case E

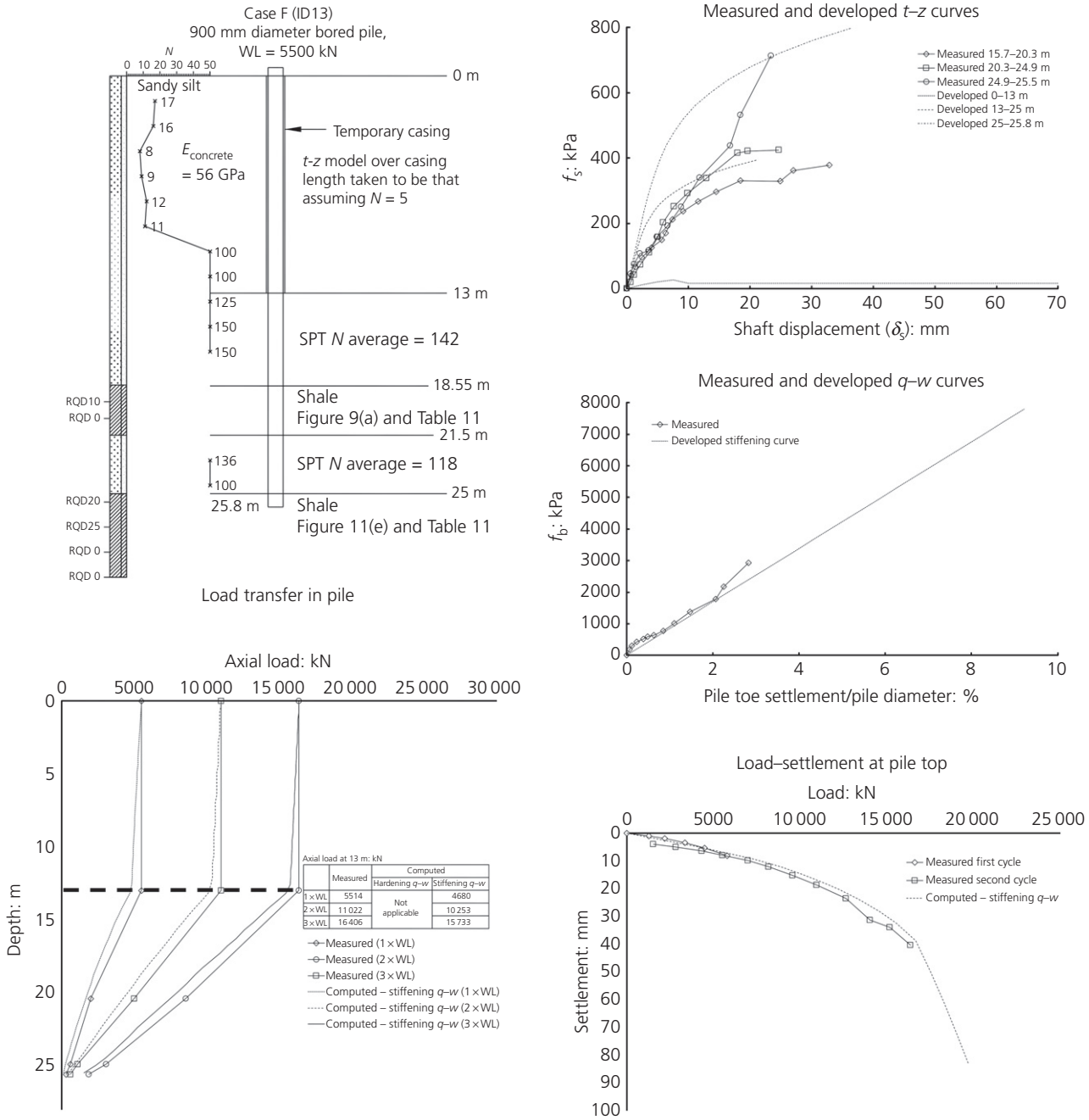

Figure 24. Application of proposed *t–z* and *q–w* – case F

(*b*) K_s values from the test data show that shaft resistance parameters reduce from more than 5.0 at low SPT N values to 2.0 at SPT N greater than 100. Commonly adopted present-day design parameters are conservative.

(*c*) The ultimate shaft resistance factors α_c and α_q from the authors' data when put together with Kulhawy and Phoon's data for rock cover the full range of rock strength (and therefore the entire weathering profiles) with q_u from 0.02 to 80 MPa. Broadly the same correlation of ultimate shaft resistance with strength holds for the full strength range from 0.02 MPa to 80 MPa, albeit with scatter.

(*d*) Strain softening shaft resistance is prevalent for SPT N below 30. Strain hardening is prevalent for SPT $N > 30$.

(*e*) The ultimate base resistance values plotted against q_{bu} are similar to that by Zhang and Einstein (1998) except for the lower bound line.

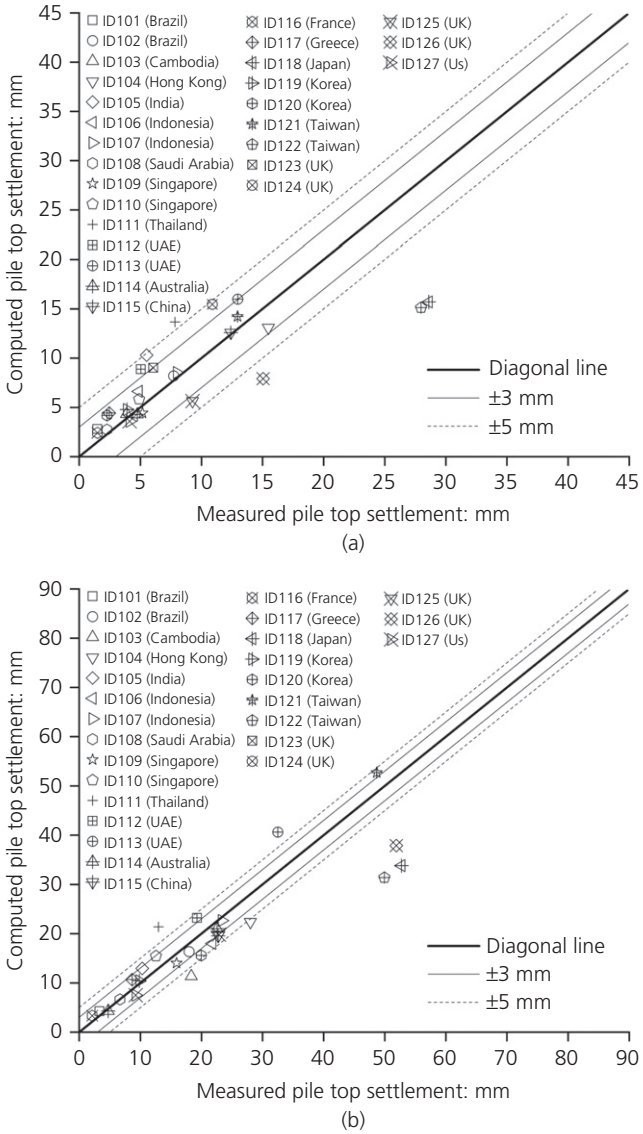

Figure 25. Computed and actual pile top settlement at: (a) half test load; (b) test load

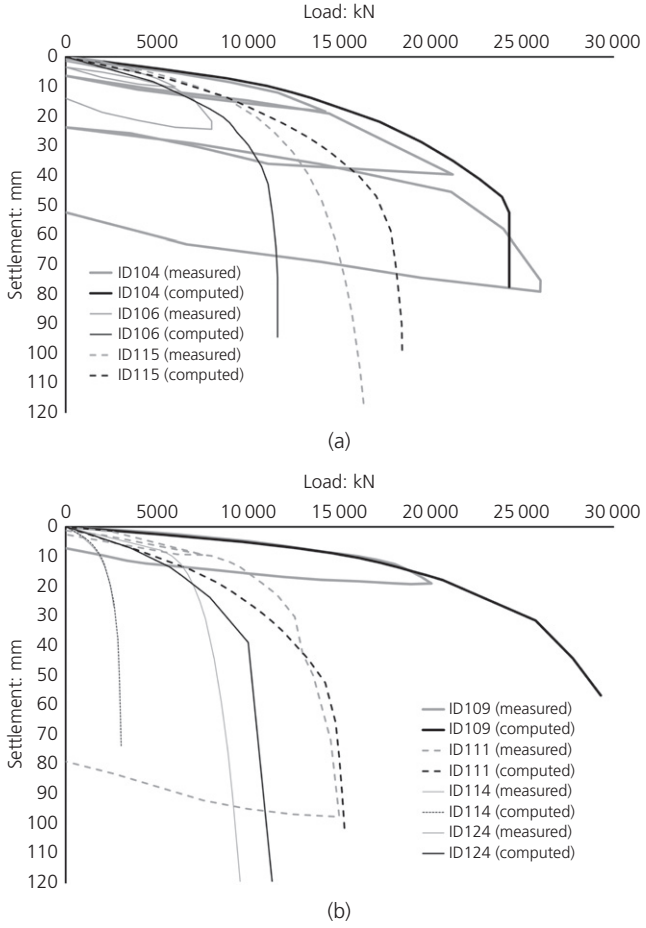

Figure 26. (a) Computed and actual pile load–settlement curves for pile ID104, 106 and 115. (b) Computed and actual pile load–settlement curves for pile ID109, 111, 114 and 124

(*f*) The Tsai (1988) and Ramberg and Osgood (1943) models were used to develop *t–z* curves. The former is used for strain softening shaft resistance behaviour, the latter for strain hardening behaviour that is prevalent for SPT $N > 30$.

(*g*) Two types of *q–w* curves were observed, namely, strain hardening and stiffening, wherein the stiffness increases with pile toe movement. The Ramberg and Osgood (1943) model is used for both strain hardening and stiffening pile toe behaviour.

(*h*) Parameters for the models for different soil and rock strengths and rock types were derived from the test data and are presented in this paper.

(*i*) The model was tested against 35 of the 100 test piles, cases for which the piles were loaded into the non-linear range with encouraging results.

(*j*) Testing of the model was extended to 27 test pile data from all over the world; the results were encouraging, especially for piles within the tropics. The model did not fare as well for piles in chalk, alluvial sand and shales outside the tropics.

Acknowledgement

The authors acknowledge Lee Siang Kai of Glostrext Sdn. Bhd. for making available the results of about 40 instrumented test piles.

Appendix 1

See Table 19 for summary of the test piles.

Appendix 2

See Table 20 for description of 27 test piles.

Table 19. Instrumented test piles (database)

ID	Description	Diameter: m	*L*: m	Socket length in grades I, II and III: m	Pile toe material	Formation	WL: MN	Test load: MN	Settlement at maximum test load: mm
1	P. Ramlee PTP1, KL. Ω^	0.9	31.5	0	*N* 53 ClSi	LSF	5.55	7.20	86.51↓
2	P. Ramlee PTP2, KL. Ω^	0.9	39.4	3.7	GI/II L	LSF	5.55	15.26	28.39↓
3	P. Ramlee PTP3, KL. Ω^	0.9	43.0	0	*N* 173 ClSi	LSF	5.55	8.11	54.01↓
4	Kerinchi PTP1, KL. Ω*	0.9	33.1	0	*N* 125 SaSi	KHF	6.30	18.53	27.39
5	Mas B. PTP1, KL. ψ*	2.5	56.0	0	*N* 188 Si	KHF	21.89	30.65	105.00
6	Mas B. PTP2, KL. ψ*	1.35	33.85	8.4	GI/II Sc	Schist	8.00	20.00	6.00
7	Tropicana PTP2, Sel. Ω*	0.9	45.7	3.9	GI/II G	GF	6.53	16.31	41.70
8	Tropicana PTP1, Sel. ψ*	1.8	24.0	4.5	q_u = 20 MPa G	GF	11.10	22.20	3.50
9	Kelana J. S. 2, KL. ψ*	1.0	21.8	3.3	q_u = 9.55 MPa G	GF	3.79	11.36	21.00
10	9 Seputeh, KL. Ω*	1.0	20.9	2.1	GIII SAs	Sandstone	6.78	20.34	39.00
11	Sky Suite, KL. Ω^	1.5	40.9	4.2	GI/II L	LSF	18.75	37.64	39.12
12	Jalan S. Ismail, KL. ψ*	1.2	20.0	0	*N* 167 SaCl	KHF	5.04	10.08	26.80
13	Lot D, K. Sentral, KL. Ω*	0.9	25.8	7.3	GI Sh	Shale	5.50	16.39	40.52
14	Elite Pavilion, KL. Ω*	0.9	63.1	1.1	GII/II L	LSF	5.56	13.00	76.16
15	KL Eco City, KL. Ω*	0.9	16.0	0	*N* 200 SaSi	KHF	5.55	14.04	21.47
16	JKG Jalan R. Laut, KL. Ω*	1.0	18.5	2.5	GI/II L	LSF	6.00	19.32	30.80
17	Tradewinds, KL. Ω*	0.9	24.8	1.8	GI L	LSF	5.55	16.90	38.88
18	Hampshire, KL. Ω*	1.0	57.1	13.4	GIII L	LSF	6.40	17.57	24.24↓
19	Lot 4 City One, KL. Ω*	1.2	10.1	2.7	GI L	LSF	8.67	17.02	4.94
20	Presint 2, Putrajaya. Ω*	0.9	22.5	2.5	GIII SAs	Shale	5.55	14.51	21.65
21	KL Pavilion, KL. Ω*	0.75	50.6	0	*N* 34 SaSi	LSF	3.30	9.90	42.52
22	KLCC Convention, Center, KL. Ω*	1.0	27.2	0	*N* 167 ClSi	Shale	5.50	10.34	47.80
23	KLHC, KL. Ω*	0.8	26.7	2.4	GI/II L	LSF	4.17	5.89	57.00
24	Seputeh, KL. Ω*	1.2	26.4	3.0	GI Sc	Schist	9.89	30.28	33.53
25	Bangsar Village, KL. Ω*	0.9	26.6	0	*N* 136 SaSi	KHF	4.70	14.00	26.10
26	Emporis, Sel. Ω*	0.9	29.8	0.3	GIII G	GF	5.55	14.23	68.03
27	Ekotitiwangsa P97, KL. ψ*	1.8	27.7	9.0	GII/III L	LSF	10.00	20.00	11.50
28	Ekotitiwangsa P122, KL. ψ*	1.35	27.3	7.8	q_u = 9.55 MPa L	LSF	5.80	11.60	9.10
29	Stonor 3, KL. Ω*	1.5	38.0	5.0	GIII L	LSF	15.46	30.56	19.49
30	Duke 2, KL. Ω*	0.9	12.4	4.9	GII/III L	LSF	5.55	14.20	20.00
31	Platinum Park P4, KL. Ω^	1.5	19.5	0	*N* 158 ClSi	LSF	10.00	23.42	115.41
32	Kapar, Sel. Ω^	1.1	40.2	0	*N* 88 SaSi		4.50	6.45	7.10
33	Bukit Damansara, KL. Ω^	0.9	25.1	0	*N* > 100 SaSi	GF	5.30	13.11	20.57
34	Platinum Park, KL. Ω^	1.8	31.0	4.0	GI/II L	LSF	22.50	45.63	20.39
35	Istana, KL. Ω^	1.2	18.0	0	Soft toe		11.31	8.88	61.49
36	Bangsar South, KL. Ω^	1.0	22.7	8.1	GII/III SIs	KHF	5.50	16.63	19.54
37	Platinum Park P3, KL. Ω^	1.8	37.0	2.7	GI/II L	LSF	22.00	44.04	24.63
38	Site E P2, Johore. Ω*	1.5	45.5	0	*N* 429 Sa	OA	15.00	30.11	57.69
39	Jalan Ampang, KL. Ω^	1.2	37.5	65	GIII L	LSF	9.80	19.44	16.92
40	Site C P2, Johore. Ω*	0.9	60.5	0	*N* 55 Sa	OA	6.30	14.01	42.89
41	Kelantan. Ω^	1.5	58.0	0	*N* 37 Sa		6.80	7.74	80.44
42#	Desa P. City, KL. Ω^	1.05	17.8	0	GIII G	GF	7.50	16.80	100.91
43	Chi Tze Kepong, KL. Ω^	0.9	16.5	1.5	GII/III L		5.00	14.94	16.17
44	Kemaman, Terengganu. Ω^	1.0	52.0	0	*N* 200 SaSi		6.27	10.85	13.74
45#	Bangi, Sel. Ω^	0.6	15.0	0	*N* 200 SaSi		3.60	7.58	43.82
46	Uptown 1, Sel. Ω^	0.9	38.3	3.2	GIII G	GF	6.30	16.52	70.35
47	Site E P1, Johore. Ω*	1.5	50.6	0	*N* 100 Sa	OA	17.67	30.24	22.86
48	Taman Tun, KL. Ω^	0.75	27.3	2.3	GIII G	GF	3.00	6.10	38.78
49	Gua Musang 1, Kelantan. Ω^	0.9	21.3	3.5	GI/II L	LSF	6.30	14.61	12.21
50	Gua Musang 2, Kelantan. Ω^	1.0	12.2	3.9	Soft toe	LSF	7.80	12.00	4.94
51	SPK Shah Alam, Sel. Ω^	1.5	21.6	0	*N* 100 SaSi		8.50	16.94	8.95
52	Kinrara, KL. Ω^	0.6	11.0	7.0	GIII Sh	KHF	3.50	6.60	20.29
53	Jade Hill 1, Sel. Ω^	0.6	22.0	0	*N* 200 ClSi		2.35	6.90	20.20
54	Ipoh, Perak. Ω^	1.0	9.7	2.3	GI/II L	LSF	4.00	12.01	5.91
55#	Jalan Robertson, KL. Ω^	1.0	27.3	0	*N* 125 ClSi		6.87	15.54	101.34
56	Cyberjaya P3, Sel. Ω^	1.2	13.5	4.0	GII/III SAs	KHF	9.00	26.97	14.25

(continued on next page)

Table 19. Continued

ID	Description	Diameter: m	*L*: m	Socket length in grades I, II and III: m	Pile toe material	Formation	WL: MN	Test load: MN	Settlement at maximum test load: mm
57	ECER, Kelantan. Ω^	1.0	9.0	3.4	GI/II L	LSF	5.50	16.51	9.08
58	Fuyuu Venture, Melaka. Ω^	11.0	52.9	0	*N* 150 SiSa		9.10	20.00	119.08
59#	PJ City, Sel. Ω^	0.9	53.9	0	*N* 115 SaSi		5.50	16.02	42.63
60	Nusajaya, Johore. Ω^	0.6	26.8	1.6	GIII/IV SAs	Sandstone	2.80	8.47	18.08
61	Site D P1, Johore. Ω*	1.2	41.5	0	*N* 88 Sa	OA	11.30	16.57	52.02
62	Hap Seng Kinrara, Sel. Ω^	1.0	30.7	0	Soft toe		7.80	21.21	63.13
63	Dengkil XMU 1, Sel. Ω^	0.9	30.1	7.6	GII/III SAs	Sandstone	5.50	14.54	34.26
64	Danga Bay, Johore. Ω^	1.0	37.5	0	*N* 100 SaSi		6.80	20.23	33.52
65	MRT Kajang, Sel. Ω^	1.2	37.0	3.8	GIII Sc	Schist	9.80	29.64	23.90
66	MRT Cheras, Sel. Ω^	0.9	44.0	0	*N* 100 SaSi	Schist	5.50	16.26	21.01
67	KLIA2, Sel. Ω^	0.75	47.3	7.1	GIII SAs	Sandstone	3.90	9.79	38.35
68	Opus 1, KL. Ω^	1.2	46.5	0	*N* 100 SaSi		9.00	26.89	40.39
69	K4 Mont Kiara, KL. Ω*	1.0	23.5	0	*N* 200 Sa	GF	5.80	11.66	19.96
70	Alor Star, Kedah. Ω^	1.05	36.2	0			7.80	5.26	44.62
71	Site C P4, Johore. Ω*	1.2	34.1	0	*N* 120 Sa	OA	11.31	19.54	69.49
72	Foresta, Penang. Ω^	1.05	10.2	4.0	GIII G	GF	5.55	11.31	4.20
73#	Gerbang Perdana TP4, Johore. Ω*	1.0	34.0	0	*N* 120 Al		5.89	15.00	64.00
74	Kapar PB2, Sel. Ω^	1.1	40.0	9.0	GIII SAs	Sandstone	4.50	8.93	9.62
75	Site C P3, Johore. Ω*	1.0	34.3	0	*N* 120 Sa	OA	7.86	14.60	18.29
76	Uptown 3, Sel. Ω^	1.2	18.7	2.0	GII/III G	GF	11.30	21.30	84.88
77	Site B P1, Johore. Ω*	1.2	51.3	0		OA	11.30	16.91	7.53
78	Jade Hill 2, Sel. Ω^	0.75	27.0	0	Soft toe		3.70	10.27	17.19
79	Dengkil XMU 2, Sel. Ω^	0.75	16.8	6.5	GIII SAs	Sandstone	3.80	6.34	55.46
80	Opus 2, KL. Ω^	1.2	46.8	0	*N* 100 SaSi		9.00	26.10	84.69
81	Persiaran Stonor, KL. ψ*	1.0	39.0	6.0	GI/II L	LSF	5.00	12.00	25.00
82	Site A P1, Johore. Ω*	0.75	47.0	0	*N* 21 SaSi	OA	4.40	6.24	73.04
83	Site A P2, Johore. Ω*	1.0	50.5	0	*N* 34 SaSi	OA	5.22	11.06	104.03
84	Site A P3, Johore. Ω*	1.0	40.0	0		OA	7.86	12.50	11.26
85	Site A P4, Johore. Ω*	0.75	55.7	0	*N* 27 SaSi	OA	4.40	8.17	26.16
86	Site A P5, Johore. Ω*	0.75	40.1	0	*N* 79 Sa	OA	4.40	8.15	20.07
87	Site C P1, Johore. Ω*	1.0	48.2	0	*N* 40 Sa	OA	7.86	14.97	24.61
88	Kg. Berembang Ampang, Sel. Ω^	0.9	34.4	9.4	GI/II L	LSF	5.50	16.76	14.00
89	Uptown 4, Sel. Ω^	1.2	22.8	6.0	GI/II G	GF	11.30	29.65	40.13
90	Jln Semangat P.J., Sel. Ω^	0.9	22.9	7.9	GII/III G	GF	6.30	18.63	35.81
91	118, KL. Ω^	1.2	53.8	0	*N* 100 Si	KHF	12.00	28.69	49.47
92	KL 100 Tower, KL. Ω^	1.5	57.0	0	*N* 200 SiSa		16.50	31.05	155.43
93	RMM Bukit Jalil, KL. Ω*	1.0	12.8	0	*N* 214 SaSi		6.10	13.45	59.30
94	Exact location not known. ψ*	1.5	14.9	4.6	GI/II L	LSF	7.50	22.50	12.00
95	Exact location not known. ψ*	1.5	22.8	7.8	GIII SAs	Sandstone	6.63	13.25	1.60
96	Exact location not known. ψ*	1.2	31.9	5.4	GII/III SAs	Sandstone	5.65	16.95	44.00
97	Exact location not known. ψ*	1.5	28.2	6.5	GIII SAs	Sandstone	8.75	17.50	3.30
98	Jalan S. Ismail P13, KL. ψ*	2.8	68.8	0	*N* 375 SaSi	KHF	27.46	54.91	32.00
99	Jalan S. Ismail P34, KL. ψ*	1.2	44.9	0	*N* 176 SaSi	KHF	5.04	10.08	31.00
100	Eaton Residence, KL. ψ*	1.5	19.5	4.6	GII/III L	LSF	8.75	17.50	9.20

L, length; WL, working load; KL, Kuala Lumpur; Sel, Selangor; Ω, maintained load test; ψ, bi-directional load test; LSF, limestone formation; GF, granite formation; OA, old alluvium; KHF, Kenny Hill sedimentary formation; #, pile plunged in load test; ↓, settlement measured at cut off level; *, conventional strain gauge; ^, Glostrext system; *N*, SPT *N* blow count; Cl, clay; Si, silt; Sa, sand; Al, alluvium with rock fragments; L, limestone; G, granite; Sc, schist; Sh, shale; SAs, sandstone; Sis, siltstone; q_u, unconfined compressive strength; GI, grade I rock; GII, grade II rock; GIII, grade III rock; MN, megaNewton

Table 20. Piles (outside database) for model testing

ID	Project site	Authors	Diameter: mm	Max. test load, P_{max}: kN	Pile length: m	Socket length: m	Type of rock at base	Measured		Estimated	
								Settlement at 0.5× P_{max}: mm	Settlement at P_{max}: mm	Settlement at 0.5× P_{max}: mm	Settlement at P_{max}: mm
101	Brazil	Albuquerque *et al*. (2009)	400	601	12	0	SPT *N* 10 clayey sandy silt.	1.49	3.32	2.81	4.24 (T)
102	Brazil	Prediction Event at Araquari (Brazil)	1000	8544	24.1	0	SPT *N* 18 clayey sand	7.73	17.98	8.19	16.34 (H)
103	Cambodia	Peou (2011)	1000	8513	31	0	SPT *N* 62 hard clay	3.88	18.34	4.33	11.36 (S)
104	Hong Kong	Terence (2000)	1320	26 000	25.5	1.9	GIII Grandorite	15.48	28.02	13.09	22.39 (H)
105	India	Gupta (2012)	1000	10 218	25	0	SPT *N* 30 sand	5.51	10.31	6.62	12.96 (H)
106	Indonesia	Widojoko (2012)	800	8000	39	0	SPT *N* > 50 clayey silt	4.87	21.78	7	18.00 (H)
107	Indonesia	Wijanto *et al*. (2017)	1200	24 381	85.5	0	Volcanic alluvial fans	7.99	23.33	8.53	22.65 (H)
108	Saudi Arabia	Ahmed (2011)	800	4715	16	0	SPT *N* 81 silty clay	2.28	6.67	2.75	6.65 (H)
109	Singapore	Leung (1996)	1400	20 040	16	5.5	GIII/IV siltstone	5.18	15.92	4.42	14.01 (H)
110	Singapore	Chin (1996)	800	9240	24	0	SPT *N* > 100 silty sand	4.90	12.55	5.83	15.45 (H)
111	Thailand	Thasnanipan *et al*. (1998)	1000	14 988	46.51	0	SPT *N* 40 dense sand	7.84	12.96	13.67	21.37 (H)
112	UAE	Russo *et al*. (2013)	1500	60 071	55.15	46.45	GIII/IV calcareous sandstone	5.04	19.27	8.87	23.20 (H)
113	UAE	Poulos and Davis (2005)	900	29 885	40	5	Calcisiltite	12.98	32.51	15.98	40.61 (H)
114	Australia	Pells and Turner (1979)	450	2627	7.2	6.7	GII/III fresh to completely weathered shale	4.76	22.57	4.29	21.02 (T)
115	China	Raithel *et al.* (2009)	1000	16 357	48	0	SPT *N* 60 silty clay	12.40	22.75	12.58	19.54 (H)
116	France	Reiffsteck (2009)	500	1310	12	0	SPT *N* 26 clay	1.50	2.15	2.42	3.35 (H)
117	Greece	Pitilakis *et al*. (1988)	1000	5061	40	0	SPT *N* 80 sandy gravel	2.47	8.65	4.42	10.67 (H)
118	Japan	Hirayama (1990)	2000	40 729	40	0	SPT *N* 30 sand	28.60	52.73	15.71	33.82 (H)
119	Korea	Kim *et al*. (1999)	1500	22 332	32.7	8	GIII granite-gneiss	3.90	9.84	4.78	10.43 (H)
120	Korea	Kim *et al*. (1999)	760	4879	5	5.4	GIII shale	2.29	19.96	4.19	15.57 (H)
121	Taiwan	Lin *et al*. (2017)	1500	34 189	45.7	7.1	GIII/IV sandstone/shale	12.95	48.70	14.22	52.70 (T)
122	Taiwan	Moh *et al*. (1993)	1500	20 412	16.6	3.8	GIII shale	27.97	49.94	15.12	31.38 (H)
123	United Kingdom	Martin and Budden (2016)	750	9563	37	0	London Clay	6.05	99.98	9.02	29.89 (S)
124	United Kingdom	Raison (2017)	600	5201	20.6	6.1	Soft chalk	10.89	61.46	15.46	— (H)
125	United Kingdom	Cole (1977)	1060	6726	8.5	1.9	GIII mudstone/sandstone	9.20	22.86	5.64	19.80 (H)
126	United Kingdom	Mallard and Ballantyne (1977)	1145	10 820	8.6	8.6	Sound chalk	15.05	51.90	7.91	37.87 (ST)
127	United States	O'Neill *et al*. (1996)	1070	6623	6	5	Glacial till (IGM)	4.12	9.22	3.59	7.50 (T)

Remarks – H, hardening *q–w*; S, stiffening *q–w*; ST, soft toe; T, tension pile

REFERENCES

Ahmed AAM (2011) *Investigation of Pile Foundations in the Al Hasa Area, Saudi Arabia*. PhD thesis, University of Portsmouth, Portsmouth, UK.

Albuquerque PJR, Paschoalin Filho JA and Carvalho D (2009) Behaviour of continuous flight auger piles subjected to uplift load tests in unsaturated diabasic soil. In *Deep Foundations on Bored Piles and Augered Piles* (Van Impe WF and Van Impe PO (eds)). Taylor & Francis Group, London, UK, pp. 197–203.

Aurora RP and Reese LC (1977) Field test of drilled shafts in clay shale. *Proceeding of 9th International Conference on Soil Mechanics and Foundation engineering, Tokyo, Japan*, pp. 371–376.

Bohn C, Alexandre LDS and Frank R (2017) Development of axial pile load transfer curves based on instrumented load tests. *Journal of Geotechnical and Geoenvironmental Engineering* **143(1)**: 1–15.

Carter JP and Kulhawy FH (1988) *Analysis and design of drilled shaft foundations socketed into rock*. Cornell University, Ithaca, NY, USA, Electric Power Research Institute Report EL 5918.

Caruba P (1997) Skin friction of large-diameter piles socketed into rock. *Canadian Geotechnical Journal* **34(2)**: 230–240.

Chang MF and Broms BB (1991) Design of bored piles in residual soils on field-performance data. *Canadian Geotechnical Journal* **28(2)**: 200–209.

Chin JT (1996) Back-analysis of an instrumented bored pile in Singapore old alluvium. *Proceedings of 12th Southeast Asian Geotechnical Conference, Kuala Lumpur, Malaysia* (Franks CAM (ed.)). The Institute of Engineers, Selangor, Malaysia and Southeast Asian Geotechnical Society, Bangkok, Thailand, vol. 1, pp. 441–446.

Cole KW (1977) *Rock-socket Piles at Coventry Point, Market Way, Conventry. Piles in Weak Rock*. The Institute of Civil Engineers, London, UK.

EGGS (Engineering Group of The Geological Society) (1990) Geological Society Engineering Group working party report, tropical residual soils. *Quarterly Journal of Engineering Geology and Hydrogeology* **23(1)**: 4–101.

Fleming WGK, Weltman AJ, Randolph MF and Elpson WK (2008) *Piling Engineering*. 3rd Edition, John Wiley & Sons, New York, NY, USA.

Frank R (1984) *Etudes Théoriques de Fondations Profondes et d'Essais en Place par Autoforage dans les LPC et Résultats Pratiques (1972–1983)*. Laboratoire Central des Ponts et Chaussées, Paris, France, *Rapport de Recherche LPC No. 128* (in French).

Frank R (2017) Some aspects of research and practice for pile design in France. *Proceedings of the International Conference on Advancement of Pile Technology and Pile Case Histories, Bali, Indonesia* (Rahardjo PP and Hutapea BM (eds)). Universitas Katolik Parahyangan, Bandung, Indonesia, vol. 1, pp. 1–15.

Glos GH and Briggs OH (1983) Rock sockets in soft rock. *Journal of Geotechnical Engineering Division, ASCE* **109(4)**: 525–535.

Goeke PM and Hustard PA (1979) Instrumented drilled shafts in clay-shale. *Symposium on Deep Foundation* (Fuller EM (ed.)), ASCE National Convention, Atlanta, GA, USA, pp. 149–164.

Gupta RC (2012) Hyperbolic model for load tests on instrumented drilled shafts in intermediate geomaterials and rock. *Journal of Geotechnical and Geoenvironmental Engineering* **138(11)**: 1407–1414.

Gupta S, Sundaram R and Gupta S (2012) Quality assurance for deep bored piles – a case study. *Proceedings of Indian Geotechnical Conference, Delhi, India*. Indian Geotechnical Society, Delhi, vol. 1, pp. 609–611.

Gupton C and Logan T (1984) Design guidelines for drilled shafts in weak rock in South Florida. *Annual Meeting of South Florida Branch of ASCE*. Preprint.

Hanifah AA and Lee SK (2006) Application of global strain extensometer (GLOSTREX) method for instrumented bored piles in Malaysia. *Proceedings of 10th International Conference on Piling and Deep Foundations, Amsterdam, the Netherlands* (Lindenberg J, Bottiau M and Tol AFV (eds.)). Deep Foundations Institute, Hawthorne, NJ, USA, pp. 669–676.

Heydinger AG and O'Neill M (1986) Analysis of axial pile–soil interaction in clay. *International Journal for Numerical and Analytical Methods in Geomechanics* **10(4)**: 367–381.

Hirayama H (1990) Load–settlement analysis for bored piles using hyperbolic transfer functions. *Soils and Foundations* **30(1)**: 55–64.

Horvath RG and Kenney TC (1979) Shaft resistance of rock-socketed drilled piers. *Proceedings of Symposium on Deep Foundations, America Society of Civil Engineers Annual Convention*. ASCE, Atlanta, GA, USA, pp.182–214.

Horvath RG, Kenny TC and Kozicki P (1983) Methods of improving the performance of drilled pier in weak rock. *Canadian Geotechnical Journal* **20(4)**: 758–772.

Hummert JB and Cooling TL (1988) Drilled pier test, Fort Collins Colorado. *Proceeding of 2nd International Conference on Case Histories in Geotechnical engineering*, St. Louis, MO, USA, vol. 3, pp. 1375–1382.

Jubenville MD and Hepworth RC (1981) Drilled pier foundations in shale – Denver Colorado area, Drilled Piers and Caisson. *Proceeding of Session at the ASCE National Convention, St. Louis, MO, USA*, ASCE, New York, NY, USA, pp. 66–81.

Kim SI, Jeong SS, Cho SH and Park IJ (1999) Shear load transfer characteristics of drilled shafts in weathered rocks. *ASCE Journal of Geotechnical and Geoenvironmental Engineering* **125(11)**: 999–1010.

Kulhawy FH and Phoon KK (1993) Drilled shaft side resistance in clay soil to rock. In *Proceedings of the Conference on Design and Performance of Deep Foundations: Pile and Pier in Soil and Soft Rock* (Nelson PP, Smith TD and Clukey EC (eds)). American Society of Civil Engineers, New York, NY, USA, Geotechnical Special Publication No. 38, pp. 172–183.

Kulhawy FH, Prakoso WA and Akbas SO (2005) Evaluation of capacity of rock foundation sockets. In *Proceeding of 40th US Symposium in Rock Mechanics* (Chen G, Huang S, Zhou W and Tinucci J (eds)). American Rock Mechanics Association, Alexandria, VA, USA, pp. 635–642.

Leung CF (1996) Case studies of rock-socketed piles. *Geotechnical Engineering Journal* **27(1)**: 51–67.

Leung CF and Ko HY (1993) Centrifuge model study of piles socketed in soft rock. *Soils and Foundation, Tokyo, Japan* **33(3)**: 80–91.

Lin SS, Lu FC, Kuo CJ, Su TW and Mulowayi E (2014) Axial capacity of barrette piles embedded in gravel layer. *Journal of Geoengineering* **9(3)**: 103–107.

Lin SS, Liao JC, Balasubramaniam AS and Lin YK (2017) Comparison Between The Tensile Behaviors of Rock-Socketed Barrette and Drilled Shaft. *Proceedings of the 19th International Conference on Soil Mechanics and Geotechnical Engineering, ICSMGE 2017* (Lee W, Lee JS, Kim HK and Kim DS (eds)), Seoul, Republic of Korea, pp. 2805–2808.

Mallard DJ and Ballantyne JL (1977) *The Behaviour of Piles in Upper Chalk at Littlebrook D Power Station, Piles in Weak Rock*. The Institute of Civil Engineers, London, UK.

Martin J and Budden D (2016) Pile tests to justify higher adhesion factors in London clay. *Geotechnical Engineering* **169(2)**: 121–128.

Moh ZC, Yu K, Toh PH and Chang MF (1993) Base and shaft resistance of bored piles founded in sedimentary rocks. *Proceeding of 11th Southeast Asian Geotechnical Conference, Singapore* (Lee SL, Yong KY and Chow YK (eds)). Southeast Asian Geotechnical Society, Bangkok, Thailand, pp. 571–576.

Ng CWW, Yau TLY, Li JHM and Tang WH (2001) New failure criterion for large diameter bored piles in weathered geomaterials. *ASCE Journal of Geotechnical and Geoenvironmental Engineering* **127(6)**: 488–498.

O'Neill MW, Townsend FC, Hassan KM, Buller A and Chan PS (1996) *Load Transfer for Drilled Shafts in Intermediate Geomaterials*. Federal Highway Administration, McLean, VA, USA, p. 194, Report No. FHWA-RD-95-172.

Orpwood TG, Shaheen AA and Kenneth RP (1989) Pressuremeter evaluation of glacial till bearing capacity in Toronto, Canada. *Foundation Engineering: Current Principle and Practice* (Kulhawy FH (ed.)), ASCE, Reston, VA, USA, vol. 1, pp. 16–28.

Pells PJN (1999) State of practice for the design of socketed piles in rock. *Proceedings of 8th Australia New Zealand Conference on Geomechanics, Hobart, Australia* (Vitharana N and Colman R (eds)). Australian Geomechanics Society, NSW, Australia. pp. 308–327.

Pells PJN and Turner RM (1979) Elastic solutions for the design and analysis of rock-socketed piles. *Canadian Geotechnical Journal* **16(3)**: 481–487.

Peou S (2011) *Paper Research of Piles Foundation in Phnom Penh Capital of Cambodia*. Faculty of Civil Engineering, National Polytechnic Institute of Cambodia, Phnom Penh, Cambodia.

Pitilakis K, Tsotsos ST and Hatzigogos T (1988) Pile tests on bored piles in Greece. In *Deep Foundations on Bored Piles and Augered Piles* (Van Impe WF (ed.)). Taylor & Francis Group, London, UK, pp. 545–552.

Poulos HG and Davids A (2005) Foundation design for the emirates twin towers, Dubai. *Canadian Geotechnical Journal* **42(3)**: 716–730.

Radhakrishnan R and Leung CF (1989) Load transfer behaviour of rock-socketed piles. *Journal of Geotechnical Engineering, ASCE* **115(6)**: 755–768.

Raison C (2017) *Pile Design to BS EN 1997-1:2004 (EC7) and the National Annex*. University of Birmingham, Birmingham, UK.

Raithel M and Kirchner A (2009) Foundation of a high speed railway track by comparing different pile load tests. In *Deep Foundations on Bored Piles and Augered Piles* (Van Impe WF and Van Impe PO (eds)). Taylor & Francis Group, London, UK, pp. 285–291.

Ramberg W and Osgood W (1943) *Description of Stress–Strain Curves by Three Parameters*. National Advisory Committee for Aeronautics, University of Washington, Seattle, WA, USA, Technical Notes, No. 902.

Randolph MF (2007) PIGLET Analysis and Design of Pile Groups, Version 5.1. The University of Western Australia, Crawley, Australia, Technical Manual.

Randolph MF and Wroth P (1978) Analysis of deformation of vertically loaded piles. *Journal of Geotechnical Engineering Division* **104(12)**: 1465–1487.

Reiffsteck P (2009) ISP5 Pile prediction revisited, contemporary topics in in situ testing, analysis and reliability of foundations. *Proceedings of International Foundation Congress & Equipment Expo '09 (IFCEE '09), Orlando, FL, USA* (Iskandar M, Degra F, Laefer DF and Hussein MH (eds)). ASCE, Reston, VA, USA, pp. 19–26. Geotechnical Special Publication No. 186.

Reese LC and O'Neill MW (1988) *Drilled shafts: construction procedures and design methods*. Publication FHWA-HI-88-042, Federal Highway Administration, Washington, DC, USA.

Reynolds RT and Kaderbeck TJ (1980) Miami limestone foundation design and construction. *Journal of Geotechnical Engineering Division, ASCE*, **107(7)**: 859–872.

Rosenberg P and Journeaux N (1979) Friction and end bearing tests on bedrock for high capacity socket design. *Canadian Geotechnical Journal* **13(3)**: 324–333.

Rowe RK and Armitage HH (1984) *The design of piles socketed into weak rock*. University of Western Ontario, Ontario, Canada. Report GEOT-11-84.

Rowe RK and Armitage HH (1987) A design method for drilled piers in soft rock. *Canadian Geotechnical Journal* **24(1)**: 126–142.

Russo G, Poulos HG and Small JC (2013) Re-assessment of foundation settlements for the Burj Khalifa, Dubai. *Acta Geotechnica* **8(1)**: 3–15.

Seidel JR and Collingwood B (2001) A new rock socket roughness factor for prediction of rock socket shaft resistance. *Canadian Geotechnical Journal* **38(1)**: 138–153.

SSC (Singapore Standards Council (2003) CP4: 2003: Code of practice for foundations. Singapore Standards, SPRING Singapore, Singapore.

Stroud MA (1974) The standard penetration test in insensitive clays and soft rocks. *Proceeding of 1st European Conference on Penetration Testing*. Swedish Geotech Society, Stockholm, Sweden, vol. 2, Part 2, pp. 367–375.

Terence LYY (2000) *Capacity and Failure Criteria of Bored Piles in Soils and Rocks*. MPhil thesis, The Hong Kong University of Science and Technology, Hong Kong.

Thasnanipan N, Tangseng P and Anwar MA (1998) Large diameter bored piles in multi-layer soils of Bangkok. In *Deep Foundations on Bored Piles and Augered Piles* (Van Impe WF (ed.)). Taylor & Francis Group, London, UK, pp. 511–518.

Thorne CP (1980) The capacity of piers drilled in rock. *Proceedings of International Conference on Structural Foundations on Rock, Sydney, Australia*. AA Balkema, Rotterdam, the Netherlands, pp. 223–233.

Thompson RP and Leach BA (1988) The application of the SPT in weak sandstone and mudstone rocks. *Proceeding of the Penetration testing in the UK, Geotechnology Conference, Institute of Civil Engineers, Birmingham, UK*. Thomas Telford, London, UK, pp. 83–86.

Toh CT, Ooi TA, Chew HK, Chee SK and Ting WH (1989) Design parameters for bored piles in a weathered sedimentary formation. *Proceeding of 12th International Conference on Soil Mechanics and Foundation Engineering, Rio de Janeiro, Brazil*. AA Balkema, Rotterdam, the Netherlands, vol. 2, pp. 1073–1078.

Tsai WT (1988) Uniaxial compressional stress–strain relation of concrete. *Journal of Structural Engineering* **114(9)**: 2133–2136.

UFRGS (Universidade Federal do Rio Grande do Sul) (2017) *Prediction Event at Araquari (Brazil) Test Site*. See https://www.ufrgs.br/araquari-ets/ (accessed 10/10/2019).

Vijayverjiya VN (1977) Load–movement characteristics of piles. *Port'77: 4th Annual Symposium of the Waterway, Port, Coastal and Ocean Division*. ASCE, Long Beach, CA, USA, vol. 2, pp. 269–284.

Webb DL (1976) The behaviour of bored piles in weathered diabase. *Geotechnique* **26(1)**: 63–72.

Widojoko L (2012) Validation study of simplified soil mechanics method design with Kentledge pile loading test of bored pile. *Proceedings of 1st International Conference on Engineering and Technology Development (ICETD 2012)*. Universitas Bandar Lampung, Lampung, Indonesia, pp. 204–210.

Wijanto B, Sengara IW, Cahyandi B, Prakoso WA and Jusmelia W (2017) Design, construction, and performance of long deep bored piles for tall building complex in Jakarta. *Proceedings of International Conference on Advancement of Pile Technologies and Case Histories, PILE 2017, Bali, Indonesia* (Rahardjo PP and Hutapea BM (eds)). Universitas Katolik Parahyangan, Bandung, Indonesia, vol. 2, pp. G8-1–G8-10.

Williams AF (1980) *The design and performance of piles socketed into weak rock*, PhD Thesis, Monash University, Clayton, VIC, Australia.

Williams AF and Pells PJN (1981) Side resistance rock sockets in sandstone, mudstone and shale. *Canadian Geotechnical Journal* **18(4)**: 502–513.

Wilson LC (1976) Tests of bored and driven piles in cretaceous mudstone at port Elizabeth, South Africa. *Geotechnique* **26(1)**: 5–12.

Wong J and Singh M (1996) Some engineering properties of weathered Kenny Hill formation in Kuala Lumpur. *Proceedings of 12th Southeast Asian Geotechnical Conference, Kuala Lumpur, Malaysia* (Franks CAM (ed.)). The Institute of Engineers, Selangor, Malaysia and Southeast Asian Geotechnical Society, Bangkok, Thailand, vol. 1, pp. 179–187.

Yeap EB (1985) Irregular topography of subsurface carbonate bedrock in the Kuala Lumpur area. *Proceeding of the 8th Southeast Asian Geotechnical Conference, Kuala Lumpur, Malaysia*. The Institute of Engineers, Selangor, Malaysia and Southeast Asian Geotechnical Society, Bangkok, Thailand, vol. 1, pp. 4-1–4-18.

Zhang L and Einstein HH (1998) End bearing capacity of drilled shafts in rock. *ASCE Journal of Geotechnical and Geoenvironmental engineering* **124(7)**: 574–584.